Chapter - 6

A simple molecular theory of smectic C liquid crystals

6.1 Introduction

In the previous chapters we have described several novel phase transitions exhibited by compounds with molecules having *longitudinal* components of permanent electric dipole moments. As described in Chapter-1, in the smectic C (SmC) phase, the constituent molecules are tilted in the smectic layers. The SmC liquid crystal is made of compounds with molecules having *lateral* components of dipole moments. There are many reports in the early literature on the synthesis of compounds that were later found to exhibit the SmC phase [1]. However, the SmC phase was given the designation originally by Sackmann and Demus [2] based on the miscibility studies and the observation of textures. In this chapter, we discuss the molecular origin of tilt in the SmC liquid crystals and develop a molecular theory of phase transitions involving SmC liquid crystals.

As described in Chapter-1, the simplest of the liquid crystalline phases exhibited by rod like molecules is the uniaxial nematic (N) which has only a long range orientational order of the long axes of the rods. Since the director $\hat{\boldsymbol{n}}$ which is a unit vector along the average orientation direction of the long axes of the rods, is *apolar* in nature, the relevant order parameter is a second rank tensor. In the smectic A (SmA) liquid crystals, the centres of mass of the rods develop a quasi long range one dimensional periodic order whose wave vector ($|\vec{\boldsymbol{q}}| = 2\pi/d$, d being the layer spacing) is parallel to $\hat{\boldsymbol{n}}$. In the smectic C (SmC) liquid crystal, the 'tilt' angle ω between $\vec{\boldsymbol{q}}$ and $\hat{\boldsymbol{n}}$ is nonzero [3] (figure-6.1)

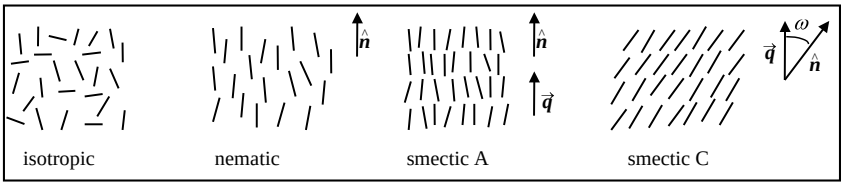

Figure - 6.1. Schematic representation of ordering of rod like molecules in the isotropic liquid and the nematic, the smectic A and the smectic C liquid crystals. The director $\hat{n}$ and the wave vector $\vec{q}$ representing the density wave along the layer normal are shown. $\vec{q}$ and $\hat{n}$ are parallel in the smectic A liquid crystals where as in smectic C liquid crystals, $\hat{n}$ is tilted with respect to $\vec{q}$ at an angle ω.

6.2 Molecular order in different types of smectic liquid crystals with molecular tilt

6.2.1 The Smectic C liquid crystal

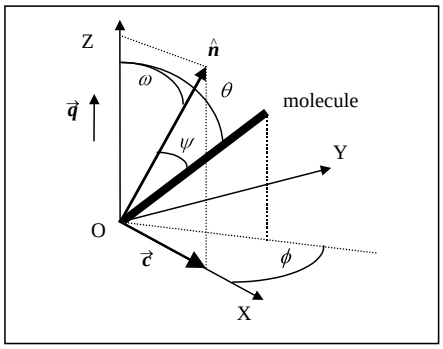

Figure - 6.2. Diagram showing the right handed rectangular cartesian coordinate system chosen with the Z axis along the layer normal. The angle between $\vec{q}$ and $\hat{n}$ is the average tilt angle ω. The Z-X plane is chosen as the tilt plane and contains $\hat{n}$. The vector $\vec{c}$ is the projection of $\hat{n}$ on the X axis. The thick line represents a given rod like molecule making the polar angle θ, the azimuthal angle ϕ and the angle ψ with $\hat{n}$.

In SmC liquid crystals, long axes of the rod like molecules have an average tilt angle ω with respect to the layer normal *i.e.*, the director $\hat{n}$ makes an angle ω with the smectic wave vector $\vec{q}$. Also, the tilt direction is the same for all the smectic layers (homoclinic). To describe the molecular orientations, we consider the right handed rectangular cartesian coordinate system with the Z axis chosen along the layer normal, *i.e.*, along $\vec{q}$ (figure 6.2). For the sake of convenience, the tilt plane is taken to be the

Z-X plane, containing the director $\hat{\boldsymbol{n}}$. The long axis of any given molecule makes an angle θ with the positive Z axis, angle ψ with $\hat{\boldsymbol{n}}$, and its projection in the X-Y plane makes the azimuthal angle ϕ with respect to the positive X axis. The relation between θ, ϕ and ψ is given by

$$\cos\psi = \cos\theta\cos\omega + \sin\theta\sin\omega\cos\phi. \qquad (6.1)$$

The molecular centres are randomly distributed within the layers in the X-Y plane as in the SmA liquid crystal.

Since the nematic director is apolar, rotating the medium by 180^0 about the Y axis results in an identical arrangement *i.e.,* there is a two fold axis of symmetry along the Y axis. Also, the Z-X plane which contains the director $\hat{\boldsymbol{n}}$ is a mirror plane of symmetry. These two symmetries together represent a point of inversion about the origin O. Hence the medium can not sustain any net polarisation.

6.2.2 Other smectic liquid crystals with molecular tilt

It has been recently found [4] that some compounds exhibit the smectic phase in which the direction of vector $\vec{\boldsymbol{c}}$ of the successive layers is opposite *i.e.,* it has anticlinic symmetry (SmC_{alt}). The suffix 'alt' stands for 'alternate' *i.e.,* the inlayer projection of $\hat{\boldsymbol{n}}$ is along the positive and the negative X directions in successive layers. The liquid crystal still can not sustain any net polarisation. A very interesting type of smectic liquid crystal (SmC*) results if the molecules are chiral. In the SmC* liquid crystals, each layer still has a two fold axis of symmetry along the Y axis, but there is no orthogonal mirror plane. The medium exhibits ferroelectric polarisation of the layers in the direction perpendicular to the tilt plane. However, due to chiral interactions, the direction of polarisation develops a gradual twist from layer to layer *i.e.,* it becomes helical about the Z axis and the structure is heli-electrical [3]. Since the polarisation vector tends to align with an external electric field, the helix can be unwound by applying an electric field perpendicular to the Z axis. The molecular ordering in the unwound SmC* resembles that of the SmC, but the medium is ferroelectric. The helix can also be unwound by placing the SmC sample in a thin cell (thickness $\approx 2\mu$m) whose surfaces are in the Z-X plane. Such a surface stabilised ferroelectric liquid crystal (SSFLC) exhibits a very useful electro optic effect when placed between appropriately oriented crossed polarisers. The field of view is dark

when the incident light is linearly polarised along $\hat{\boldsymbol{n}}$. If the direction of the applied electric field is reversed, the direction of the average tilt is also reversed, resulting in a change of 2ω in the direction of $\hat{\boldsymbol{n}}$. Since the optic axis is parallel to the director, this results in a corresponding change in the direction of the optic axis of the medium and the field of view becomes bright. The dark field can be restored by rotating the cell by an angle 2ω about the direction of electric field. This helps in the measurement of ω optically. Also, this leads to a wide range of applications in electro-optic display devices. Hence, a large number of such compounds have been synthesised and studied.

The hexatic smectic liquid crystals have an additional inlayer bond orientational order having a hexagonal symmetry. Depending on the nature of the inlayer order, the liquid crystal is termed as SmF, SmI *etc.* [1]. These are not considered in the present thesis.

We will develop a simple molecular theory of the simplest of the tilted smectic liquid crystals, *i.e.,*SmC liquid crystal. Such a medium is also biaxial. This is described in the next section.

6.2.3 Biaxiality in the SmC liquid crystals

The smectic A liquid crystals have the optic axis along $\hat{\boldsymbol{n}}$ *i.e.,* along the layer normal and the medium is cylindrically symmetric about $\hat{\boldsymbol{n}}$. The medium is uniaxial, even if the molecules are biaxial. In the SmC liquid crystal, the medium has a layered structure of the molecules as in SmA but the molecules are tilted in one direction *i.e.,* in the Z-X plane (see figure 6.2). Hence, the refractive index or the dielectric constant measured along the X and Y directions give different values. The difference between these two values represents the asymmetry *about the Z-axis* or the biaxiality of the structure which is quite large ($\sim 10^{-2}$).

It should be further noted that, in the SmC liquid crystals, the fluctuations in the orientation of the long axes of the individual molecules are *not* equally probable in all directions around the *director*. The ϕ fluctuations (Goldstone mode) or the inlayer fluctuations cost less energy, whereas the θ fluctuations cost more energy (soft mode) since they tend to alter the layer spacing. Hence, the averaged projection of the molecular long axes along the Y direction fluctuates a little more than that in a

direction orthogonal to the Y- $\hat{\boldsymbol{n}}$ plane. In other words, the medium does not have cylindrical symmetry *about the director*. This leads to a *weak* biaxiality (~10^{-4}) [5] about the director and hence it is neglected in many theoretical calculations.

In the next section we give a brief review of some of the experimental results relating to the SmC liquid crystals.

6.3 Review of some important experimental results

6.3.1 Measurement of the tilt angle ω

As explained in section 1.2.2 (chapter-1), X-ray diffraction from smectic liquid crystals show quasi Bragg peaks that imply a periodic structure. Using these, the layer spacing of the smectic liquid crystal can be calculated. In the monolayer SmA liquid crystals, this calculation gives a layer spacing $d_A \approx l$ where l is the molecular length. X-ray diffraction from the SmC liquid crystals, gives the layer spacing $d_C < l$, since the molecules are tilted. The tilt angle ω can be obtained using the relation

$$\cos\omega = d_C/d_A. \tag{6.2}$$

These measurements of layer spacings give the average molecular tilt. The tilt angle can also be measured optically in SmC* liquid crystals as explained in section 6.2.2. Since the polarisability anisotropy is due to the aromatic core in the molecular structure, optical measurements give the tilt of only the molecular core. It is known that the tilt values obtained by these two methods are not always the same [6]. This implies that the core and the chain of the molecules can have different tilt angles with respect to the layer normal.

6.3.2 Typical molecular structures of compounds exhibiting the SmC liquid crystals: the significance of dipoles

As already discussed in chapter-1, molecules with an aromatic core and end chains having more than 5 carbon atoms are usually required to stabilise the SmA liquid crystal. The aromatic cores tend to overlap due to the strong dispersion interactions. The end chains separate the cores leading to the formation of the layered structure. Some additional features are essential for the molecules to be *tilted* in a smectic layer. The most common feature is the presence of a *lateral* component of the

electric dipole moment. This is possible when the molecule has a *polar* bond in the end chain and/or in the core. The dipole moments of some typical polar bonds are given in table 1.1 (chapter-1).

An alkyl chain has only C-H bonds whereas an alkoxy chain has an additional oxygen atom, thus forming a polar bond (figure 6.3). The dipole moments due to such bonds are at an angle to the molecular long axis. Hence, they have components both parallel and perpendicular to the molecular long axis.

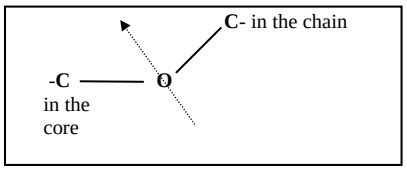

Figure - 6.3. Diagram illustrating the dipole moment due to an alkoxy chain attached to an aromatic core. Since the oxygen atom is more electronegative than the carbon atom, electrons are shifted towards the oxygen atom. This results in two dipoles in the direction O → C. The resultant dipole moment is indicated by the arrow with the dotted line.

Studies during 1980's and early 1990's have been recently reviewed by Goodby [7a]. We can see that, the presence of a *lateral* component of electric dipole moment in the molecule is the most common feature for the medium to exhibit the SmC phase. We give below some examples of compounds to illustrate the common features. In the following molecular structures, the carbon and the hydrogen atoms are not shown. Here, (L, R) represent alkyl or alkoxy chains with (*m*, *n*) carbon atoms respectively.

(a) Azobenzenes : [8]

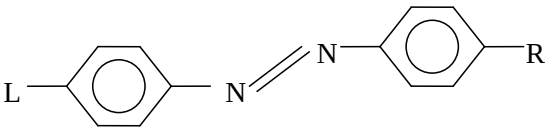

The N–C bonds contribute two equal and opposite dipoles which do not have lateral components. Hence if both L and R are alkyl chains, the compound does not exhibit the SmC phase (*m* = *n* = 3 to 10). When R is replaced by an alkoxy chain (*m* = *n*+1 = 8 and 9), the compounds show 2nd order SmA-SmC transition. If both L and R are alkoxy chains (*m* = *n* = 8 and 9), the compounds show 1st order N-SmC transition. If the central azo link is also replaced by an azoxy group (*eg.*, HOAB-**h**eptyl**o**xy **a**zoxy **b**enzene), it shows a stronger 1st order N-SmC transition(*m* = *n* = 7) [9]. This shows that, if the number of lateral dipoles is increased, the tendency to form

the SmC liquid crystal also increases. In general, an addition of a dipolar group at the end of the molecule has a similar effect [10].

(b) TB*n*A - Terepthal-bis-*n*-alkyl aniline [11].

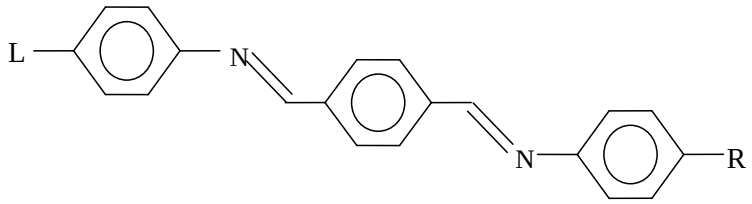

In this molecule, the C=N bonds contribute two lateral dipoles. Hence, in general, even if L and R are alkyl chains, the compounds (m = n = 8 and 10) exhibit SmC liquid crystals.

(c) Pyrimidines - [12]

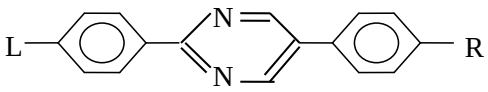

The compound shows the SmC phase when R is an alkoxy chain, for different combinations of m (varying between 3 and 10) and n(varying between 4 and 10).

d)Alkoxybenzoates- [13], (denoted as n OPEPOm)

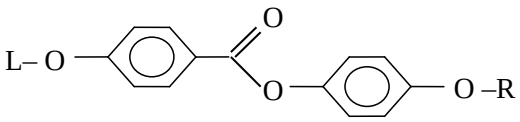

The two lateral components of dipole moment due to the COO bond almost cancel out. The compound shows SmC phase as it has alkoxy chains, for different combinations of m and n, each varying between 6 and 18.

6.3.3 Possible phase sequences involving SmC liquid crystals

Experimental studies on several homologous series and mixtures show that, in general the following phase sequences are possible on cooling-

(a)I-N-SmA-SmC (see figure 6.4)

(b)I-N-SmC

(c)I-SmA-SmC

(d)I-SmC

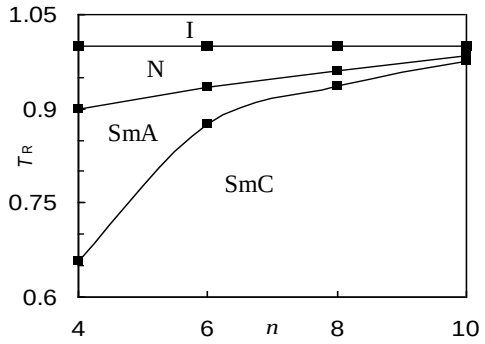

Figure - 6.4. Experimental phase diagram for the homologous series of compounds 10OPEPO*n* (see structure d, section 6.3.2) plotted using data in reference [13]. $T_R = T/T_{NI}$ where T_{NI} is the N-I transition temperature. The solid lines are guides to the eye.

Of these the I-N, I-SmA and I-SmC transitions have first order character and the N-SmC, the N-SmA and the SmA-SmC can have first or second order character.

6.3.4 Effect of chain length and dipole moment of the molecules on the SmC-SmA phase transition

When the temperature of the SmC liquid crystal is increased, usually the tilt angle ω continuously decreases to zero as the SmC phase undergoes a *second* order transition to the SmA phase. There is no heat of transition but, the specific heat plotted as a function of temperature shows a strong peak in the SmC phase near the transition point and a negative jump on transition to the SmA phase. On the other hand, if the SmC phase undergoes a *first* order transition to the SmA phase, initially ω decreases continuously but abruptly jumps to zero at the transition point. There is a finite heat of transition and the peak in the specific heat is not as pronounced as at a second order SmC-SmA transition. We give below some examples to illustrate the effect of chain length of the molecules on the nature of the transition and on the variation of ω and specific heat with temperature.

Studies on TB*n*A (Terepthal-bis-*n*-alkyl aniline, see structure (b) in section 6.3.2 above) show that [11] TBOA (O stands for -octyl *i.e.*, n = 8) exhibits a 2nd order SmA-SmC transition whereas the longer homologue TBDA (D stands for -decyl *i.e.*, n = 10) exhibits a 1st order SmA-SmC transition. In a mixture of the two, as the concentration of the longer homologue (TBDA) is increased, the nature of the SmA-SmC transition changes over from 2nd order to 1st order (see table 6.1) Further, the temperature range of the SmA phase decreases.

Table 6.1.

Material [11]	SmA range in ^{0}C	Jump in ω
TBOA	10.0	0
10% of TBOA in TBDA	2.9	8.9^0
TBDA	1.8	12.8^0

Studies on pyrimidines (structure (c) in section 6.3.2 above) show that [12] as the chain length is increased, the heat of the 1st order SmA-SmC transition increases and temperature range of the SmA phase decreases, if the end chains are *symmetric* (figure 6.5).

Studies [13] on the alkoxybenzoates (structure (d) in section 6.3.2 above) with symmetric and unsymmetric end chains shows that as the chain length is increased, the temperature variation of the tilt angle ω becomes steeper in case of the 2nd order SmA-SmC transition.

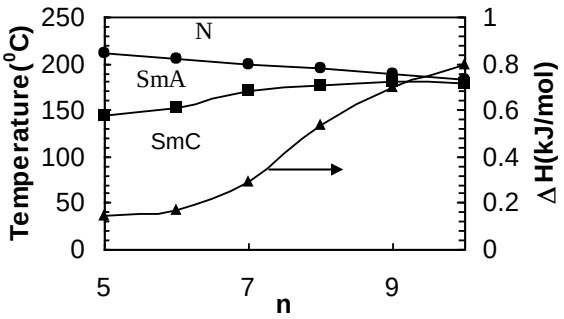

Figure - 6.5. Variation of the heat of transition (ΔH) and the temperature range of SmA phase as the chain length increases for pyrimidines having symmetric end chains with n carbon atoms, plotted using values from reference [12]. The solid lines are guides to the eye.

Studies [14] on binary mixtures of methyl-chloropentanoyloxy heptyloxy biphenyl (with strong dipole moment) and heptyloxy decyloxyybenzoate (with weak dipole moment) show that as the relative concentration of the strongly polar compound is increased, the temperature range of SmA decreases and the second order SmC-SmA transition changes to first order. As noted by Liu *et al* , [15] this can be interpreted as due to an increase in the *effective* molecular transverse dipole moment.

In general, experiments clearly indicate that, as the chain length in a homologous series or the concentration of a longer homologue in a mixture is increased, the temperature variation of the tilt angle ω becomes steeper in case of the 2^{nd} order SmA-SmC transition, the transition changes over to 1^{st} order (indicated by the jump in ω at the transition) and then becomes a stronger 1^{st} order transition (indicated by the increase in the heat of transition). Also, the temperature range of the SmA phase decreases. The same trend is seen even when the magnitude of the transverse dipole moments of the constituent molecules is increased.

6.4 Review of the theoretical work on SmC liquid crystals

Many phenomenological theories have been developed for SmC liquid crystals to account for the tricritical behaviour of the SmC-SmA transition, the nature of the N-SmA-SmC point *etc*. The experimental data on the temperature variations of the tilt angle ω and the specific heat associated with the transition are often analysed in comparison with the phenomenological Landau theory to find the Landau coefficients and the critical exponents. There have also been many attempts to account for the molecular origin of the tilt in the SmC phase. In this chapter, we develop a molecular theory of SmC liquid crystals. Close to a second order SmC-SmA transition, the expression for free energy in our molecular theory of the SmC phase is reduced to a form analogous to that in the Landau theory. In the next sub section, we review the Landau theory of the SmC-SmA transition.

6.4.1 Description of the SmC-SmA transition using the Landau theory

As described in section 1.6 (chapter-1), the phenomenological Landau theory is based on the assumption that, close to a second order transition, the free energy can be expressed as a power series in the relevant order parameter(s). de Gennes proposed a Landau theory of SmC liquid crystals taking ω as the order parameter. Normally,

terms with ω^2 and ω^4 are sufficient to explain the usual second order SmC-SmA transition. However, Huang and Viner [16] found this to be inadequate for the analysis of the specific heat data of the SmC-SmA transition in some compounds. They extended the Landau theory and showed that a sixth order term in ω is necessary for this purpose. This model is briefly described below.

The free energy of the SmC phase is written as

$$F = F_0 + at\omega^2 + b\omega^4 + c\omega^6 \tag{6.3}$$

where F_0 is the free energy of the SmA phase, a, b and c are positive constants for a second order transition, $t = (T - T_{CA})/T_{CA}$ where T_{CA} is the SmC-SmA transition temperature and ω is the tilt angle which is the order parameter. Note that t is negative for $T<T_{CA}$ (SmC phase). Minimising F with respect to ω gives

$$\omega = 0, \qquad T>T_{CA} \text{ (SmA phase)}$$

$$\omega^2 = \frac{b}{3c}\left[-1 + \left(1 - \frac{3t}{t_0}\right)^{1/2}\right], \quad T<T_{CA} \text{ (SmC phase)}, \tag{6.4}$$

where

$$t_0 = b^2/ac. \tag{6.5}$$

Substituting these in equation 6.3, and using the standard relation

$$C_P = -T\frac{\partial^2 F}{\partial T^2} \tag{6.6}$$

gives the following expressions for the heat capacity,

$$C_P = C_{0,} \qquad T>T_{CA} \text{ (SmA phase)}$$

$$C_P = C_0 + \frac{a^2(1+t)}{2bT_{CA}(1 - 3t/t_0)^{1/2}}, \quad T<T_{CA} \text{ (SmC phase)} \tag{6.7}$$

where C_0 is the background heat capacity obtained from F_0.

The jump in the specific heat at the SmC-SmA transition obtained by substituting $T=T_{CA}$ (and hence $t = 0$) in equation 6.7 is

$$\Delta C_P = C_P - C_0 = \frac{a^2}{2bT_{CA}}. \tag{6.8}$$

At $t = -t_0$, equation 6.7 gives,

$$\frac{C_P - C_0}{T} = \frac{a^2}{4bT_{CA}^2} = \frac{1}{2}\frac{\Delta C_P}{T_{CA}} \quad (6.9)$$

Hence, the parameter t_0, in the reduced temperature scale, represents the full width at half maximum of the $(C_P - C_0)/T$ vs T curve.

As shown in section 1.6.3 (chapter-1), with a positive coefficient for the sixth order term in the free energy expansion ($c>0$ in equation 6.3), the transition is first order in nature when the coefficient of the fourth order term is negative ($b<0$ in equation 6.3), while $b>0$ results in a second order transition and $b = 0$ represents the tricritical point at which the nature of the transition changes over from first order to second order. For a second order transition, if $b>>c$, then t_0 is large (see equation 6.5). From equation 6.4, it can be seen that, close to the SmC-SmA transition, *i.e.*, for $|t| << t_0$, this results in a simple mean field behaviour, with

$$\omega \propto t^{1/2}. \quad (6.10)$$

The tricritical point is approached when the value of b is decreased. If $b \sim c>0$, then t_0 is small and even for temperatures close to the SmC-SmA transition $|t| >> t_0$. From equation 6.4, it can be seen that, this results in a tricritical behaviour, with

$$\omega \propto t^{1/4}. \quad (6.11)$$

Thus, t_0 also represents the cross over temperature from the mean field to the tricritical behaviour.

6.4.2 Experimental determination of the Landau coefficients

Since the value of t_0 is crucial in deciding the tricritical behaviour of the SmC-SmA transition, it has to be determined very accurately. The value of t_0 can be independently obtained by fitting the tilt angle data to equation 6.4 or the heat capacity data to equation 6.7. The tilt angle measurement requires a well aligned sample. It is much easier to obtain high quality heat capacity data than high quality tilt angle data. Hence, the parameter t_0 is measured from the heat capacity data. The tilt angle data is later used to find the other Landau coefficients. Usually, for a second order transition showing a simple mean field behaviour, $c<<b$, the coefficients of higher powers have still smaller values and $t_0 \sim 10^{-1}$ [17]. Lien and Huang [16b], on analysing the experimental data on different compounds showing SmC-SmA

transition, found that a~10^{-3}, b~10^{-4}, c~10^{-3} (all in J/mol) and t_0 ~10^{-3}. As t_0 is very small, the SmC-SmA transition is close to the tricritical behaviour which is described by a mean field model with an unusually large sixth order term in the free energy expansion.

It is reported that the tilt angle data of a compound showing a second order SmC-SmA transition, when fitted to equation 6.4 gives [18] a fairly large value of t_0 (~10^{-1}). This compound shows a wide temperature range of the SmA phase (~60^0C) and as expected from the above theory, the temperature variation of ω is not steep (equation 6.10).

In general, for a second order SmC-SmA transition, an increase of the value of c with respect to that of b shows that the tricritical point is being approached. As described above, this trend is associated with a decrease in the temperature range of the SmA phase for compounds exhibiting N-SmA-SmC and I-SmA-SmC sequences. These experimental results suggest a change in the nature of the SmC-SmA transition from second order to first order when approaching the N-SmA-SmC and I-SmA-SmC triple points [7b]. This has also been verified for one homologous series [11].

As mentioned in chapter-1 (section 1.6.3), studies on homologous series show that, the shorter homologues show a large temperature range of the N phase and a second order SmA-N transition. For longer homologues the temperature range of the N phase decreases and also the SmA-N transition changes over to first order. This tricritical behaviour of the N-SmA transition has been successfully explained on the basis of the Landau theory using a coupling between the orientational and the translational orders. A similar coupling between the translational and the tilt orders has been used [19] to explain the tricritical behaviour of the SmC-SmA transition. However, in reference [19], the order parameter is not the tilt angle ω but it is a vector representing the extent of dipolar alignment due to freezing of molecular rotations about their long axes (see figure 6.6d in the next section). The phenomenological model [3] of SmC liquid crystal has been extended to SmC* liquid crystals including the chiral interactions.

Chen and Lubensky [20] have not introduced the tilt angle as the order parameter. They extended the Landau- deGennes theory including a term with $C_\perp$, an elastic constant against tilting of the director with respect to the layer normal. $C_\perp$ <0 favours

the SmC phase. The model is useful in analysing the X-ray diffraction data. In the $C_\perp$ vs temperature phase diagram, the model predicts a Lifshitz point at the N-SmA-SmC meeting point *i.e.*, the second order N-SmA and the SmA-SmC transition lines meet the first order N-SmC transition line. $C_\perp$ and the heat of transition of the N-SmC transition vanish at the N-SmA-SmC point.

The phenomenological models do not address the question of the molecular origin of tilt and hence are not considered here. In the next section we review some molecular theories which have been developed to account for the tilt in SmC liquid crystals.

6.4.3 Earlier molecular mean field theories of SmC liquid crystals

The nematic phase can be stabilised mainly by the hard rod packing effects at low densities in case of long rods (length to breadth ratio ~ 100). On the other hand, the anisotropic attractive interactions make a significant contribution to the orientational potential at high densities in the case of relatively short rods [3]. Indeed, a molecular theory of nematic liquid crystals developed by Maier and Saupe (MS) [21] successfully captures the qualitative features of the nematic-isotropic (N-I) transition, though it is based on the attractive intermolecular interactions only (see section 2.3, chapter-2 for a review of the theory). A quantitative comparison between theory and experiments requires the inclusion of the hard rod features of the molecules as well [3]. McMillan [22] extended the MS theory to the SmA liquid crystals (reviewed in section 3.2, chapter-3) by noting that the long alkyl chains at the two ends of the molecules favour the formation of layers, as the molecules then become polyphilic. However, his model *does not* restrict the tilt angle ω to be zero, and excluded volume effects have been shown to favour the formation of SmA [23]. Subsequently it has been shown by computer simulation studies [24] that hard rod packing effects alone can stabilise the SmA phase.

The molecular origin of the nonzero value of ω in the SmC liquid crystal has been a subject of much discussion. As explained in the section 6.3.2, the common feature of all the compounds which exhibit the SmC phase is that their molecules have permanent dipolar groups with *lateral* components. Based on this observation, McMillan developed a molecular theory of the SmC liquid crystal. In view of some

limitations of this model, many other molecular models were developed later. These models are briefly reviewed in this section.

The McMillan [25] model is based on the knowledge, at that time, that most compounds that exhibited the SmC phase had symmetric structures and dipole moments at the two ends of the central core structure. He considered compounds like di-alkoxyazoxybenzenes (similar to structure 'a' in section 6.3.2) which has three lateral dipoles. Lateral dipoles rigidly attached to the molecule on its central axis are considered, one at the molecular centre and the other two, called the *outboard* dipoles, placed above and below this at equal distances in the configuration shown in the figure 6.6a.

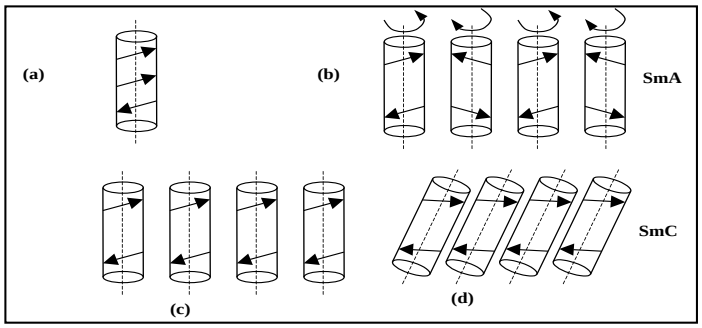

Figure - 6.6. (a) Schematic diagram showing the molecule with three lateral dipoles as proposed by McMillan. When the central dipole is much weaker than the outboard dipoles, it results in the non ferroelectric SmC phase. Hence, the central dipole is not shown in the remaining figures used to explain the mechanism of tilt in the SmC phase. (b) shows the free rotation of the molecules in the SmA phase. (c)shows the arrangement with the molecular rotations frozen with the dipoles aligned. (d) shows the tilted structure of the aligned dipoles, resulting in the SmC phase.

In the SmA phase, the molecules freely rotate about their long axes (figure 6.6b). The dipolar interactions tend to hinder the free rotation. Examining the dipole interactions in the mean field approximation, McMillan showed that, as the temperature is lowered, a transition can occur between the rotationally free to rotationally frozen states. This corresponds to the arrangement with the dipoles aligned (figure 6.6c). This creates a torque when the outboard dipoles have longitudinal components also. Hence, the molecules tilt to lower the energy of the oriented dipoles (figure 6.6d). If the central dipole is much weaker than the outboard dipoles, this results in the usual non ferroelectric SmC liquid crystals.

A model predicting a rotational freezing based purely on steric factors was proposed by Wulf [26]. He assumed a zig-zag shape for the molecules, with the end chains obliquely aligned with respect to the molecular core. It is shown that, a freezing of free rotation about the molecular long axes associated with a tilted arrangement lowers the free energy due to packing requirements.

Structural studies by Goodby *et.al* [27] show that *terminal outboard* dipoles, assumed in the McMillan model, are not essential for a SmC phase to exist. Both the McMillan and the Wulf models rely on the freezing of the molecular rotations in order to stabilise the SmC phase. NMR [28] and neutron scattering [29] measurements show that the molecules in the SmC phase are rotating about their long axes with an almost random orientational distribution, on a time scale of 10^{-11}s. Also, as noted by Goossens [30], in Wulf's model, the molecular potential used has no zig-zagness in it and hence it is not consistent with the tilt mechanism proposed.

Cabib and Benguigi [31] tried to overcome this problem by allowing the molecules to freely rotate about their long axes. They assume that the molecule has two opposite dipoles placed on the molecular long axis at equal distances from the geometric centre of the molecule. Due to random axial rotation, the perpendicular components are averaged out and only the two oppositely oriented axial components remain. When the medium has the nematic and the SmA order, the axial dipoles at the same level in the neighbouring molecules repel whereas those at different levels attract since they are oppositely oriented. Based on this, it is shown that a tilted structure lowers the energy. The model is not suitable since there are examples of compounds, whose molecules have only one central dipole, exhibiting the SmC liquid crystals [27]. Also, it is known that the *lateral* component of the dipole moment in the molecule is essential for the medium to exhibit the SmC phase as illustrated in section 6.3.2.

The molecular model widely referred to in the literature is the one proposed by Van der Meer and Vertogen. We briefly review this in the next section.

6.4.3.1 Model proposed byVan der Meer and Vertogen

Van der Meer and Vertogen [32] consider molecules freely rotating about their long axes. They argue that the permanent dipole in one molecule gives rise to an induced dipole in the neighbouring molecule. They assume the polarisability to be

concentrated at the centre of the molecule. The mutual alignment of the permanent and the induced dipoles creates the force responsible for tilting (figure 6.7) while the resistance to tilt has contributions from a combination of Van der Waal's interactions and hard core repulsions.

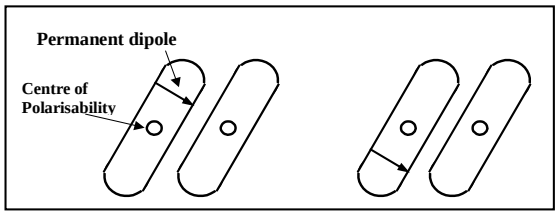

Figure - 6.7. Schematic representation of the induced dipole model showing the two possible dispositions treated with equal weightage [32].

They conclude that a transverse dipole positioned at an optimum distance from the molecular centre results in a tilted structure. A change in the molecular structure like the extension of the terminal carbon chain is taken to be equivalent to a change in the relative position of the dipoles (induced and permanent).

The model has the following drawbacks:

- In the model, the tiling force arises mainly because the permanent dipole is *acentral* while the core has a *central* and *point* polarisability. However, most liquid crystalline compounds have aromatic cores with more than one phenyl ring having a distributed probability density of electrons. Hence, it is not reasonable to take the polarisability to be concentrated at a point on the core.
- This model is not self consistent as shown by Goossens [30] since a steric contribution which has the same packing temperature 'T_P' for both the smectic and nematic phases is used.
- The number of parameters used is at least 6, some of which are themselves functions of other molecular parameters like the polarisability, dipole moment *etc.*
- Though a 'nematic' potential is used, the orientational order parameter is taken to be fixed at 0.8 in the smectic phases and it cannot hence be a self-consistent calculation. They have made a constant nematic order parameter approximation which corresponds to temperatures much below T_{NI}. As such, the SmC and SmA phases occur at temperatures well below the T_{NI}. Hence, the SmC-I and the SmA-I transitions are not described.

- The proposed effective single particle potential is quite elaborate. However it does not simply go over to the usual McMillan potential when the tilt angle $\omega = 0$. Though ω is the average tilt angle, *there is no angular variable* in the theory whose average is given by ω.
- As Van der Meer and Vertogen discuss at the end of their paper, the model for SmA to SmC transition proposed by them is *not* of an order-disorder type. However, as we mentioned in section 6.4.1, the Landau theory has been used to quantitatively analyse both the temperature dependences of the tilt angle ω as well as the specific heat implying that the transition is indeed of the order-disorder type.

Goossens [30] has critically reviewed in 1985 the above molecular theories as well as some similar ones and has shown that none of them is satisfactory. We briefly discuss some of the molecular models proposed after 1985 in the next section.

6.4.3.2 Some recent molecular models of SmC liquid crystals

Goossens [33] pointed out that the molecular quadrupoles can give rise to a tilting of molecules in smectic layers, though he did not calculate the relevant phase diagrams. Barbero and Durand [34] developed a *Landau* theory incorporating the influence of quadrupolar interactions. Sluckin *et.al.*[35] developed a molecular theory with quadrupolar interactions, but the authors themselves remark that the SmC phase is predicted to occur at higher temperatures compared to the SmA phase, which is contrary to experimental trends (see figures 6.4 and 6.5). Very recently, Giesselman *et.al.* [36] have proposed a *2-D model* analogous to ferroelectric to paraelectric transition and surprisingly they have assumed a perfect orientational order of rods, though the calculated distribution function depends on the tilt angle. Hu and Tao [37] have developed an elaborate model incorporating short range correlations, but found that the translational and orientational order parameters *decrease* in the lower temperature range of the SmC phase.

6.4.3.3 General comments and motivation for developing a new model

Based on the above review, we can make the following general comments:

- There is no satisfactory molecular theory of the SmC liquid crystal, even though a large number of experimental studies have been undertaken on the SmC and SmC* liquid crystals.
- Since there are several liquid crystals with molecular tilt, it is important to understand the molecular origin of tilt in the SmC liquid crystal which is the simplest.
- A proper molecular theory of the SmC liquid crystal, as Goossens [30] points out, must include the intrinsic biaxiality of the phase. Otherwise, the equations describe only a tilted SmA liquid crystal and not a SmC liquid crystal.
- The molecular potential used should be actually derived form the tilt mechanism proposed, or if it is assumed, it should be consistent with the mechanism proposed.
- ω is the tilt angle obtained as an *average* over an appropriate distribution function of the angles θ and ϕ subtended by the individual molecular long axes with respect to the cartesian coordinate axes (see figure 6.2). Hence, the assumption of a saturated nematic order makes the equations thermodynamically inconsistent, though it helps in simplifying the mathematical treatment.

In the next section we propose a new mechanism for the tilting of the molecules in the SmC liquid crystals.

6.5 New model for molecular tilting in SmC liquid crystals

As explained in section 6.3.2, chemical studies have shown [27,38] that molecules having at least one dipolar group with a *lateral* component is essential for the formation of the SmC liquid crystal. Looking carefully at the molecular structures, it becomes clear that, in general, the centre of this dipole is *not* on the long axis of the molecule, but is slightly shifted away from it, *i.e.*, *off-axis* by a distance ξ (see figure 6.8a). We show that this ***off axis*** lateral electric dipole moment in the molecular core is the origin of the tilting in the SmC phase.

6.5.1 Dipolar origin of tilt

As the neighbouring molecules in a smectic layer freely rotate about their long axes, at a particular mutual orientation, the lateral dipoles face each other at close proximity. This contributes to a large repulsive energy especially when the molecular

centres are at the same z' coordinate (figure 6.8a). In the configuration shown in figure 6.8b, the dipolar interaction is attractive. If the dipoles are *on* the molecular long axis, the average energy would be zero when both the molecules are allowed to freely rotate about their long axes. Since the dipoles are *off axis*, their separation in the configuration shown in figure 6.8a is less than that in figure 6.8b. Therefore the repulsive energy contribution is more than that of the attractive energy, leading to a net repulsive energy when averaged over molecular rotations. Hence, to lower the energy, the molecules tend to have a relative shift (dz') along their long axes (figure 6.8c). However, due to this shift, the attractive dispersion energy between the cores is reduced. We calculate the net interaction energy considering a pair of molecules in a smectic layer. We show that the average energy has a minimum when $dz' \neq 0$.

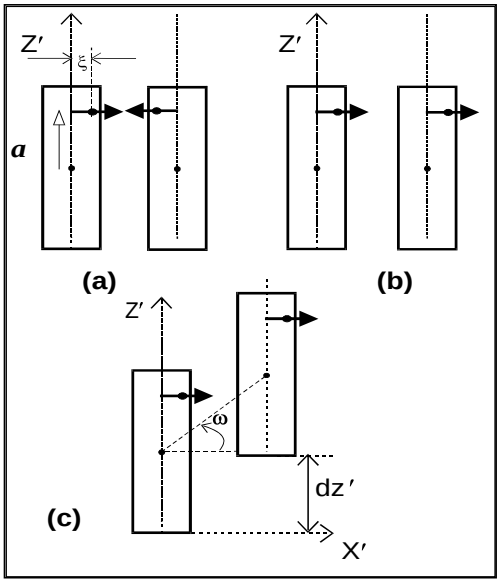

Figure– 6.8. The proposed off-axis dipolar mechanism of tilt in smectic C layers. The repulsive energy of antiparallel configuration of dipoles (a) is much larger than the attractive energy of parallel configuration (b), resulting in a relative shift of the molecules (c).

In the SmC phase, a tilt angle ω with respect to the layer normal is equivalent to the near neighbour molecules having a relative shift dz' in the tilt plane as shown in figure 6.9. In fact, figure 6.9a is obtained by rotating figure 6.9b by an angle ω. It would seem that the interaction energy can be lowered if the shift dz' occurs for all the neighbours of a given molecule. This is incompatible with the layering order, which is

consistant with a tilt only in one plane containing the layer normal, as in the usual SmC liquid crystal.

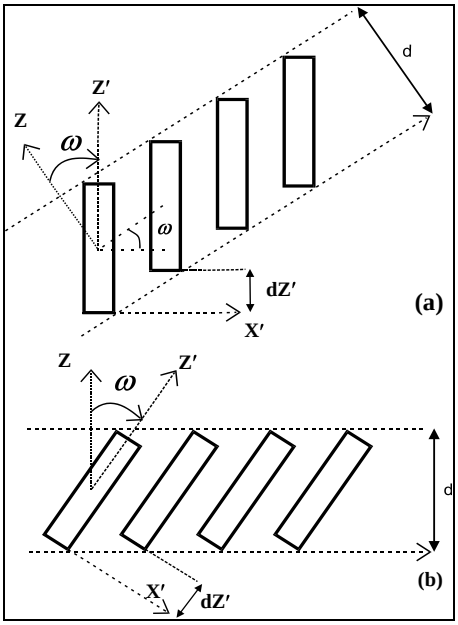

Figure- - 6.9. The mutual relative shift of molecules along Z′ shown in (a) is equivalent to a tilting of the molecules in the layers with the layer normal along Z (b).

We take into account the following factors in calculating the average intermolecular energy of near neighbours in a smectic layer:

(i) The molecules are assumed to be cylindrical rods with off axis lateral dipoles and the rods are freely rotating about their long axes. The long axes are considered to be parallel, for the purpose of the present calculation.

(ii) As the director is *apolar*, the molecules are allowed to flip about their short axes. This means that the near neighbour configurations with the $\vec{d}$ vectors (see figure 6.8a) parallel as well as antiparallel are equally probable.

(iii) The molecules tilt only in one plane, and the relative shift is zero in a plane orthogonal to the tilt plane (see figure 6.10).

(iv) The molecules also experience an attractive potential due to the dispersion interaction between the aromatic cores. This is $\propto 1/r^6$, r being the separation between

the molecular axes. This is taken to be proportional to the length of overlap [39] between the neighbours with a distributed polarisability χ.

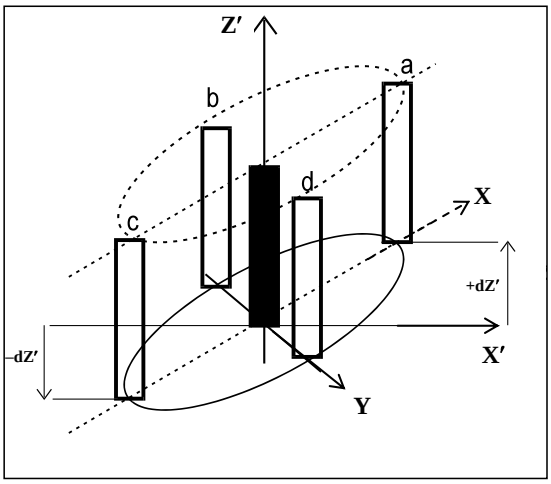

Figure – 6.10. While the averaging is done at different positions around a given molecule in a real smectic C layer, the Z′-shift is maximum in one plane (as for a and c along X) and zero in an orthogonal one (as for b and d along Y).

6.5.2 Dipole-dipole interaction energy

The notations used are shown in figure 6.11. For a given tilt ω, or equivalently, for a shift dz', the interaction energy between the 'point' permanent dipoles of the two molecules (see figure 6.11) is given by,

$$U(\phi_1,\phi_2,\omega,\Phi) = \frac{1}{4\pi\varepsilon_o}\left[\frac{\mathbf{p}_1\bullet\mathbf{p}_2}{r^3} - \frac{3(\mathbf{p}_1\bullet\mathbf{r}_{12})\,(\mathbf{p}_2\bullet\mathbf{r}_{12})}{r^5}\right] \qquad (6.12)$$

where, $\mathbf{p}_i$ is the permanent electric dipole moment of the i^{th} molecule, $\vec{a}$ the projection on the Z′-axis of the position vector of the dipole with respect to the molecular centre, $\mathbf{r}_{ij}$ the position vector of the centre of dipole moment of j^{th} molecule with respect to that of i^{th} molecule, $r = |\mathbf{r}_{ij}|$ and ε_o is the absolute permittivity of free space. For calculating the average energy, it is convenient to define the following angles (see figure 6.11).ϕ_i is the angle of $\mathbf{p}_i$ with the X′-axis, ω the angle between the X′-axis and the line joining the molecular centers and Φ the azimuthal angle with respect to the X′-axis of the projection of the intermolecular vector on the X′-Y plane.

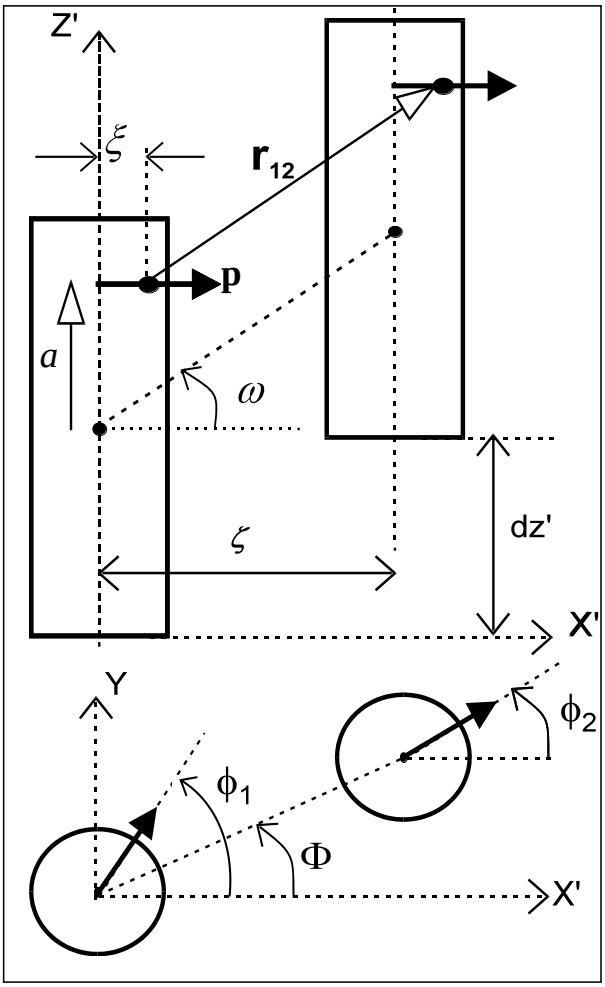

Figure – 6.11. Geometrical parameters used in the calculations of the intermolecular energy in smectic-C layers.

We consider the molecules to be parallel (↑↑) or antiparallel (↑↓) depending on the relative orientations of $\vec{a}$ of the two molecules. The average dipolar interaction energy when both the parallel (↑↑) molecules are allowed to rotate about their long axes is given by,

$$U_P^{\uparrow\uparrow}(\omega,\Phi) = \frac{1}{4\pi^2}\int_0^{2\pi} d\phi_1 \int_0^{2\pi} d\phi_2 \, f(\phi_1,\phi_2) U_P^{\uparrow\uparrow}(\phi_1,\phi_2,\omega,\Phi) \qquad (6.13)$$

where $f(\phi_1,\phi_2)$ is an appropriate angular distribution function. In the SmC liquid crystal, it is known that the molecules are almost freely rotating about their long axes. For simplicity, we consider all values of ϕ_1 and ϕ_2 to be equally probable and take $f(\phi_1,\phi_2) = 1$ while finding the average. Obviously, considering the actual distribution function can only lower the minimum energy. Since the vectors $\vec{a}$ of the near neighbours can be antiparallel at the same values of ω and Φ, a similar average for $U_P^{\uparrow\downarrow}(\omega,\Phi)$ can be defined as in equation 6.13. Including this, the average dipolar energy is,

$$U_p(\omega,\Phi) = \frac{U_P^{\uparrow\uparrow}(\omega,\Phi) + U_P^{\uparrow\downarrow}(\omega,\Phi)}{2} \tag{6.14}$$

6.5.3 Dispersion interaction between the aromatic cores

The dispersion energy between the aromatic cores depends on their polarisabilities. The aromatic cores usually consist of many phenyl rings with distributed probability density of electrons. Hence, it is reasonable to take the polarisability to be *distributed* over the length rather than being concentrated at a point on the core, and the dispersion energy depends only the overlapping length of the cores of the neighbours [39]. Therefore, the dispersion energy between the aromatic cores is written as,

$$U_D(\omega,\Phi) = -\frac{\chi_i \chi_j l h\nu}{\zeta^6} \tag{6.15}$$

where, χ_i is the distributed polarisability of the i^{th} molecule, l is the fractional length of the core laterally overlapping with that of the neighbouring molecule, h is Planck's constant, ν is the frequency corresponding to the bond ionisation energy and ζ is the lateral separation between the long axes (see figure 6.11). Hence, for a given ω and Φ the average interaction energy is

$$U(\omega,\Phi) = U_P(\omega,\Phi) + U_D(\omega,\Phi). \tag{6.16}$$

6.5.4 Average over the different relative positions of the near neighbours in a SmC layer

Within the smectic C layer, a given molecule is surrounded by a liquid like distribution of different near neighbours. All these relative positions corresponding to

different values of Φ are not energetically equivalent since in the SmC liquid crystal the molecules tilt only in the Z-X plane. For the different positions of the neighbouring molecules around the given molecule, the relative Z′-shift varies from (+dz') to (–dz') (see figure 6.10). This alters the overlapping length of the cores and hence the dispersion energy. Moreover, the separation of molecular centers is not the same in X and Y directions (see figures 6.10 and 6.11). We find the inlayer average (*i.e.*, average over Φ), by assuming the *lateral* separation between the long axes (*i.e.*, ζ in figure 6.11) to be constant. Since the inlayer distribution of the molecules is symmetric about the Z-X plane, it is enough to consider Φ varying between zero and π. Hence, for a given ω, the total interaction energy is,

$$U(\omega) = \frac{1}{\pi}\int_0^{\pi} d\Phi\, U(\omega,\Phi) \tag{6.17}$$

where we have given equal weightage to all values of Φ.

6.5.5 Values of the parameters used in the calculation

Again, for simplicity, the induced dipoles, the small contribution from chain-chain and chain-core dispersion interactions are not included in the calculations. Obviously, considering these can only lower the minimum in energy.

The following reasonable values of the parameters are used (see figure 6.11):

p = 1.5 to 4 Debye (1D = 3.33 x 10^{-30} C m).

core length = 12 Å (1Å = 10^{-10} m).

ζ = 5 Å.

ξ = 2 Å.

a in the range 0 to ±6 Å .

dz' in the range 0 to 12 Å, equivalent to $\omega = 0^0$ to about 70^0.

$\nu = 10^{15}$ Hz, equivalent to λ =300 nm; giving $h\nu/ k_B T$ =165.42 at 290K.

Also, for p =1 D and r =1Å , $p^2/(4\pi\varepsilon_0 r^3)$ is nearly 25 $k_B T$, at T = 290K, where k_B is the Boltzman constant.

For a concentrated polarisability χ = 50 Å^3 in equation 6.15 (with l = 1), we get U_D/k_BT = –26.47. But, empirical calculations of the interactions between two smectogenic (ethyl p-methoxybenzilidine aminocinnamate or MBACE) molecules by Sy and Ptak [40] show that the Van der Waals energy is only a few k_BT for full lateral overlap of the parallel molecules. Also, at the N-I transition temperature, the Maier-Saupe theory gives a value U/k_BT = –4.541, which is the average dispersion energy due to many near neighbours. For only a *pair* of molecules, the energy can be expected to be smaller than this. We find that a distributed χ =11 Å^3 gives a reasonable value of U_D/k_BT = –1.28 for l = 1 in equation 6.15. We evaluate the integrals in equations (6.13) and (6.17) numerically using the 32 point Gaussian quadrature method in double precision.

6.5.6 Variation of the average energy with respect to ω

Taking into account all the factors mentioned above, the averaged interaction energy is calculated for different values of the tilt angle ω in a smectic C layer. The averaged energy $U(\omega)$ clearly shows a minimum for a well defined tilt angle ω as shown in figure 6.12 for a =2Å and ξ = 2Å, p = 1.5 Debye. The contributions from $U_P^{\uparrow\uparrow}$, $U_P^{\uparrow\downarrow}$, and U_D after averaging over Φ are also separately shown. It can be seen that, for small values of ω, $U_P^{\uparrow\uparrow}$ is larger in magnitude than $U_P^{\uparrow\downarrow}$ as explained earlier (see figure 6.8). The minimum in $U_P^{\uparrow\downarrow}$ is lower than that of $U_P^{\uparrow\uparrow}$. This is because, when $\vec{a_1}$ and $\vec{a_2}$ are parallel, the dipoles attain the strongly repulsive configuration (figure 6.8a) twice during inlayer average (positions b and d having dz' = 0 in figure 6.10) irrespective of the ω value. On the other hand, for $\vec{a_1}$ and $\vec{a_2}$ antiparallel, the dipole of 2nd molecule is below the molecular centre and contributes only an attractive energy even for dz' = 0. We denote the ω corresponding to the minimum of $U(\omega)$ as ω_C. $U(\omega)$ has a net minimum for $\omega_C \approx 21^0$ which implies that a tilted phase is preferred. Keeping the values of a and ξ the same as above, with p = 4 Debye we get a steeper minimum at $\omega_C \approx 28^0$. In general, the position and depth of the minimum depends on the number, positions and the strength of the dipoles. This is discussed in the next section.

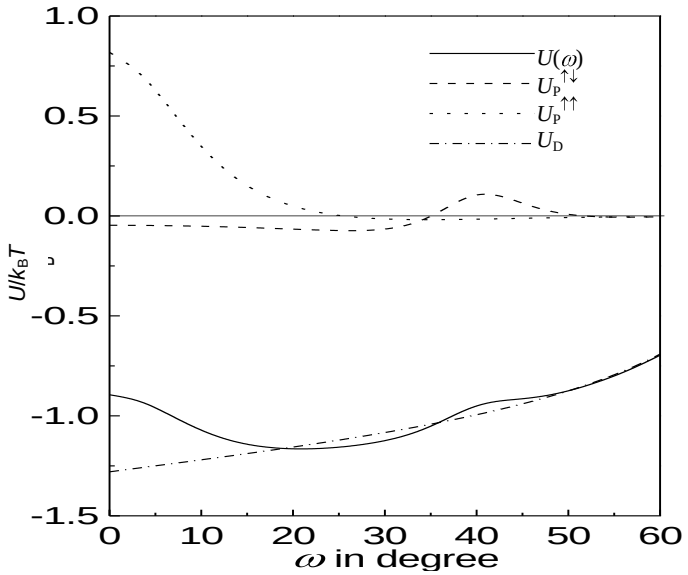

Figure – 6.12. The different contributions to the averaged energy $U(\omega)$, as a function of ω for a =2Å, ξ = 2Å and p = 1.5 Debye. The thin horizontal line corresponds to $U(\omega) = 0$.

6.5.7 Influence of the location and the number of dipoles on $U(\omega)$

We have extended our calculation to show the influence of changing the location of a single dipole on $U(\omega)$ (figure 6.13). For $a = 0$, $U(\omega)$ has only one minimum at $\omega_C \approx 24^0$ due to symmetry in $U_P^{\uparrow\uparrow}$ and $U_P^{\uparrow\downarrow}$. But, for $a \neq 0$, $U(\omega)$ can have two minima. For values of a up to about 0.7Å, the 2nd minimum is lower and leads to large values of ω_C. As can be seen from figure 6.13, ω_C (second minimum) increases a little when a is increased from 0Å to about 0.7Å. The two minima become equal when $a \approx 0.7$Å and ω_C jumps from 27.7^0 to 12.4^0 (figure 6.14). For larger values of a, the 1st minimum is lower. ω_C increases again till $a \approx 2$Å and if a is increased beyond 2Å, ω_C decreases a little (from 21^0 to 20^0 when a is increased from 2Å to 6Å, see figure 6.14). Calculations with p = 4D show that ω_C decreases from 31^0 to 29^0 when a is varied from 3.5Å to 6Å. Hence, we can conclude that, if there is only a *single* dipole, its location does not change ω significantly, unless it is located close to the molecular centre.

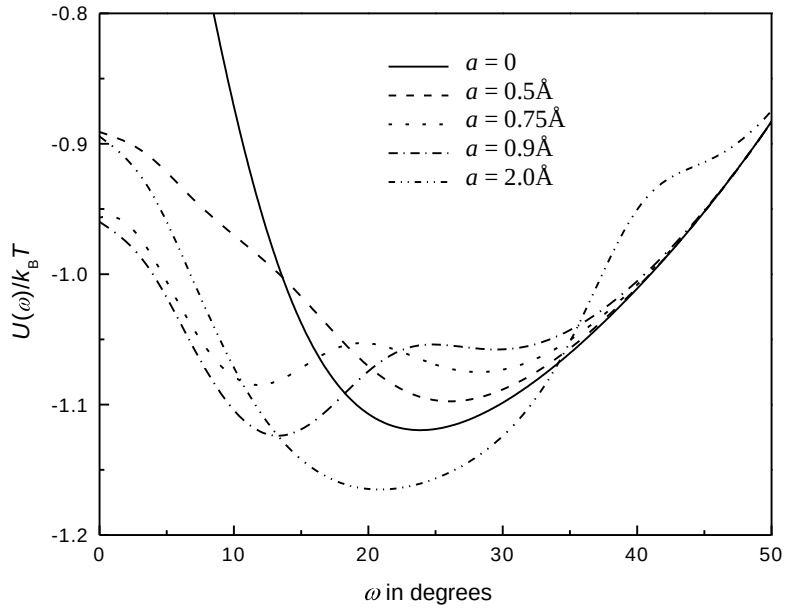

Figure – 6.13. Variation of $U(\omega)$ as a function of ω for different values of a with ξ = 2Å, p = 1.5 Debye.

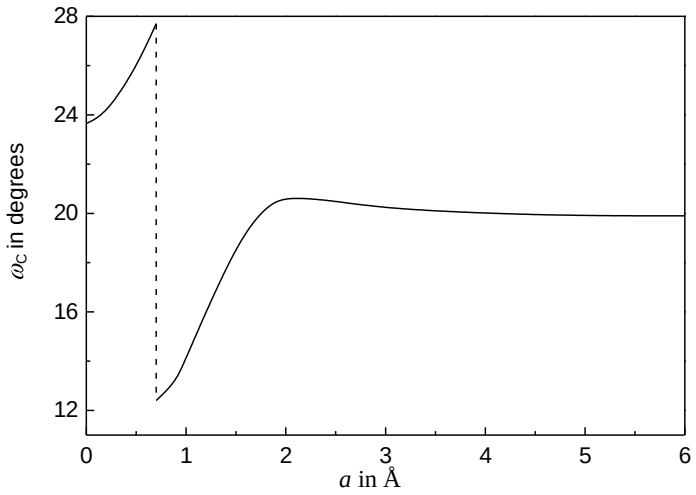

Figure – 6.14. The variation of ω_C for different values of a with ξ = 2Å, p = 1.5 Debye.

The influence of the relative location of the dipoles becomes significant when there are *two* dipoles as discussed below.

Several hundred compounds exhibiting liquid crystals with tilted molecules (SmC and SmC*) have been synthesised so far. Usually the molecules have several dipoles with various relative orientations and locations. We have studied the dependence of the averaged interaction energy on the number and the relative locations of the dipoles in the molecules. We consider two *parallel* dipoles at distances a_1 and a_2 from the molecular centre. Two *equal* dipoles symmetrically placed above and below the molecular centre results in a single minimum of $U(\omega)$ with respect to ω and this is equivalent to a single dipole of double strength at $a = 0$. When the two dipoles are unequal in magnitude and/or unsymmetrically placed with respect to the molecular centre, in general, $U(\omega)$ has four local minima with respect to ω, of which one (usually the first or the second) is the deepest. Of the two dipoles, if one is near the centre (p_1 =1.5D, $a_1 = 0$, $\xi_1 = 2$Å) and if a_2 of the other is varied from 2Å to 5Å (p_2 =1.5D, $\xi_2 = 2$Å), ω_C increases from 15^0 to 30^0 and if $p_2 = -1.5$D, ω_C increases from 25^0 to 45^0. When two antiparallel dipoles ($p_1 = -p_2$) are symmetrically placed above and below the molecular centre ($a_1 = -a_2$ and on the same side *i.e.*,$\xi_1 = \xi_2$), the net effect is $p = 0$ at the centre, resulting in lowest $U(\omega)$ for $\omega = 0$ due to the contribution from dispersion energy only.

For $a \neq 0$, as mentioned above, $U(\omega)$ has two minima in case of a single dipole and can in general have four local minima in case of two dipoles. Our calculations also show that in some cases there can be two *equal* energy minima with respect to ω. For example, as mentioned earlier, in case of a *single* dipole of strength 1.5 D, the two minima are equal for $a \approx 0.7$Å. For $p = 4$D, they are equal at $a \approx 1.1$Å. In case of *two* antiparallel dipoles on the same side of the molecule ($p_1 = -p_2 = 1.5$D, $\xi_1 = \xi_2 = 2$Å), the two minima with respect to ω become equal when a_1=0 and $a_2 = 6$Å. This suggests the possibility of a first order SmC to SmC transition involving a jump in ω. However, we have not come across any experimental observation in support of this.

6.5.8 Comparison with the experimental results

In many smectogenic compounds the molecules have two alkoxy end groups (with opposite lateral components of dipole moments) with or without a central dipole, as assumed by McMillan (figure 6.15).

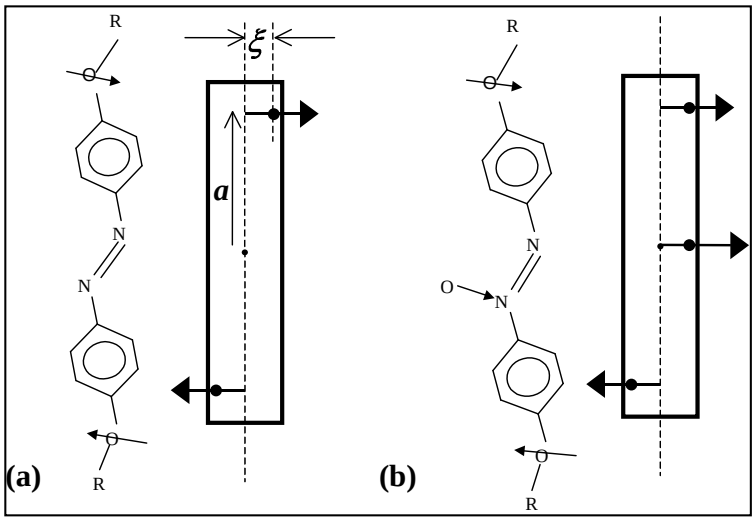

Figure - 6.15. The structural formula and the corresponding model used in our calculations of interaction energy for (a) di-alkoxy*azo*benzene and (b) di-alkoxy*azoxy*benzene. The lines with solid arrow head indicate the dipole moments, 'R' represents an alkyl chain, O and N represent oxygen and nitrogen atoms respectively. The carbon and hydrogen atoms are not shown. a and ξ define the position of the point dipole.

Synthetically, a continuous variation of a is difficult since the dipoles are usually attached to the terminal phenyl rings. A systematic study of this kind is not available for a specific comparison with our results with the variation of a. However, in case of azobenzenes [8], the influence of adding one or more dipolar groups has been specifically studied. We consider this for a comparison with the results of our calculations. The models for the molecular structures, used in our calculations of interaction energy are shown in figure 6.15. The results of the calculations are shown in figure 6.16. We compare the experimental and the calculated results in table 6.2.

Experimental studies indicate that [10], the stability of the SmC phase depends strongly on the structure of the constituent molecules. In general, molecules with stronger dipoles lead to SmC liquid crystals with larger ω and adding a terminal dipole increases the stability of the SmC phase. It can be seen that the theoretical

trends reflect the experimental ones and the origin of tilt due to the *off-axis* lateral dipoles appears to be reasonable.

Table 6.2

Experimental observations [8,9]	Results of our calculation
1. Non-polar dialkyl azo benzenes do not exhibit the SmC phase	For $p = 0$, $U(\omega)$ is lowest for $\omega = 0$ due to the contribution from dispersion energy only (U_D in figure 6.12).
2. Replacement of one alkyl group by the polar alkoxy group gives rise to both SmA and SmC phases	If there is only one dipole of strength 1.5 Debye at $a = 5$Å and $\xi = 2$Å, there is a broad minimum at $\omega \approx 19^0$ (figure 6.16a).
3. Replacement of both the alkyl groups by alkoxy groups gives rise to SmC and N phases	If there are two equal and opposite dipoles (at $a = 5$Å, $\xi = 2$Å and $a = -5$Å and $\xi = -2$Å, figure 6.15a), there is a sharper minimum at 27^0 (figure 6.16b).
4. Dialkoxyazoxy compounds exhibit N and SmC with a large value of ω [9]	A third dipole of strength 2 Debye near the molecular centre (at $a = 0$, $\xi = 2$Å, figure 6.15b) gives rise to an even sharper minimum at $\omega = 34^0$, in addition to a higher minimum at $\omega = 58^0$ (figure 6.16c).

The above discussion shows that the value of ω_C and also the shape of the curve representing the variation of $U(\omega)$ with respect to ω depend on the relative positions and the orientations of the dipoles. Hence, the general form of the tilting potential depends on the detailed molecular structure. We propose a simple single particle potential to broadly represent the general form of the variation of $U(\omega)$ with respect to ω shown in figure 6.16. This is used to develop a mean field theory of the SmC liquid crystals in the next section.

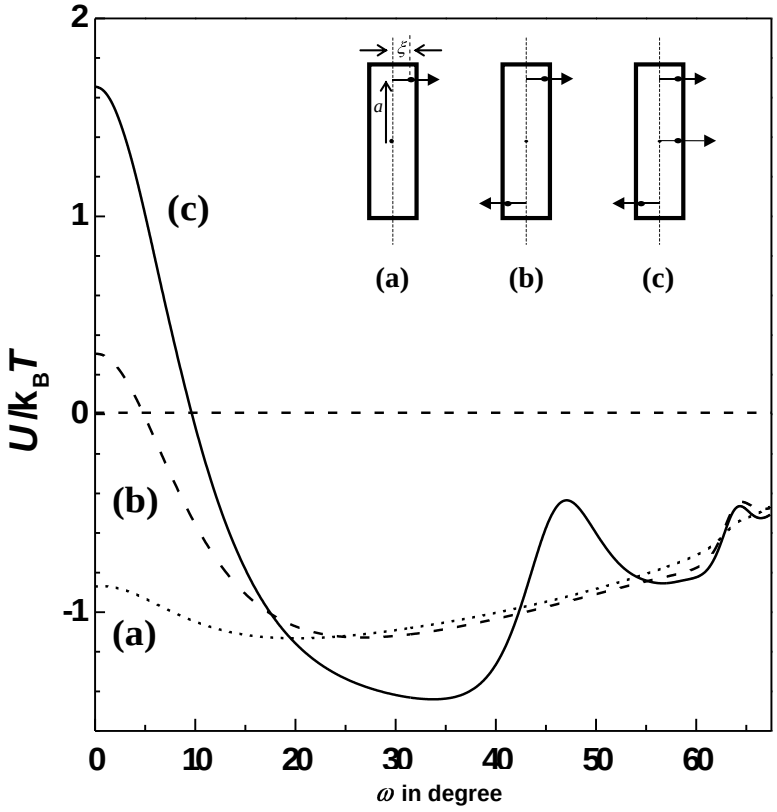

Figure – 6.16.The interaction energy U/k_BT with T=290K is plotted as a function of tilt angle ω in degrees. (a) single dipole, 1.5D, at a = 5Å, ξ = 2Å (b) two opposite dipoles 1.5D each, one at a =+5Å, ξ =+ 2Å and the other at a = – 5Å, ξ = – 2Å, (c) three dipoles, two as in (b) and one more of 2D at a =0 and ξ=2Å. Note that the net energy at the minimum is always negative.

6.6 Mean field theory of the SmC liquid crystal

6.6.1 The tilting potential

We propose a single particle tilting potential U_C considering the following points:

1. The molecular tilting is relevant only in the presence of a layering order *i.e.*,when $\tau \neq 0$. As the sign of τ depends only on the choice of origin (see figures 6.8 and 6.9), by symmetry, the tilting potential should depend on τ^2. Hence,

$$U_C \propto \tau^2. \tag{6.18}$$

2. The calculations shown in figure 6.16 indicate that the strength and the number of minima of the tilting potential depend on the detailed molecular structure. We can write,

$$U_C(\theta_i) \propto -\sum_n \beta_n \sin 2n\theta_i \tag{6.19}$$

where β_n would depend on the strength and the geometrical arrangement of the dipoles in the molecules.

3. The above calculations have been made for molecules with perfect orientational order (S=1) for the sake of simplicity. In reality, $S\neq1$ and hence the angles θ and ϕ subtended by the individual molecular long axes with respect to the cartesian coordinate axes (see figure 6.2) vary according to an appropriate distribution function. Hence, U_C is coupled to S. Since the coupling of U_C with τ has been taken into account, and τ is coupled to S as in the McMillan model for SmA phase, we do not consider the direct coupling of U_C with S.

4. The SmC medium is biaxial as described in section 6.2.3. Hence, the tilting potential depends on ϕ. This can be incorporated by writing,

$$U_C(\phi_i) \propto \cos\phi_i. \tag{6.20}$$

5. As usual in any mean field theory, the single particle potential depends on the extent of the relevant order in the medium. If η is the SmC order parameter, we can write,

$$U_C \propto \eta. \tag{6.21}$$

In view of these, a general single particle tilting potential which is consistent with the biaxial symmetry of the medium can be written as:

$$U_C(\theta_i, \phi_i) \propto -\sum_n \beta_n \eta_n \tau^2 \sin 2n\theta_i \cos\phi_i \tag{6.22}$$

where β_n would depend on the strength and the geometrical arrangement of the dipoles in the molecules, $\tau = \langle\cos(2\pi z/d)\rangle$ is the translational order parameter with z the position of the molecular centre along the layer normal $\hat{z}$ and d the layer spacing, the smectic C order parameter $\eta_n = \langle\sin 2n\theta\cos\phi\rangle$ with θ_i and ϕ_i the polar and azimuthal angles of the long axis of the i^{th} molecule with respect to the coordinate

axes (see figure 6.2). For the sake of simplicity, we restrict the calculation to n = 1, which favours a maximum tilt angle of 45^0. The effect of taking into account n =2 will be discussed later (see section 6.8.1).

This potential has to be added to the layering potential which is effective even in the absence of a tilt.

6.6.2 The layering potential

We have already introduced in chapter-3 (section 3.2), the McMillan theory of the SmA liquid crystals based on a layering potential. As described in chapter-3 (section 3.4.1.2), following Katriel and Kventsel [41], the decoupled form of the McMillan potential is,

$$U_M(\psi_i, z_i) = -U_o[1+\alpha\tau\cos(2\pi z_i/d)]\,S(3\cos^2\psi_i - 1)/2 \qquad (6.23)$$

where the nematic order parameter $S = \langle 3\cos^2\psi - 1\rangle/2$, ψ being the angle between the long axis of the molecule and $\hat{\boldsymbol{n}}$, $U_o = 4.541 k_B T_{NI}$, the strength of orienting (MS) potential expressed in terms of the N-I transition temperature T_{NI} (see chapter-2, section 2.3) and the Boltzmann constant k_B. The McMillan parameter

$$\alpha = 2\exp[-(\pi r_o/d)^2] \qquad (6.23a)$$

is a measure of the strength of the layering potential, r_o/d being the ratio of the length of the core to the layer spacing. For simplicity we assume that the core and chain tilt by the same angle in the SmC liquid crystal and hence the value of α is taken to be independent of tilt. However, it is often mentioned in the literature that the tilt angle of the core is more than that of the chain and the calculations including this effect are discussed later (see section 6.8.2).

The theory based on equation (6.23) however does not specify the relative orientation between the director and the layer normal and all 'tilted' smectic A configurations have the same energy. The smectic A phase is favoured due to excluded volume effects. In chapter-5, we considered the excluded volume effects in our calculations with a saturated orientational order but the effect of tilting was not included. In the previous chapters, our interest was only in describing the SmA-N transition and the variation of excluded volume with respect to tilt was not important. In developing a model for the SmC liquid crystals, it is necessary to include the

excluded volume effect depending on the tilt, which ensures that the SmA phase can also be stable.

6.6.3 Excluded volume contribution to stability against tilt

To demonstrate the effect of tilting on the excluded volume, we consider elongated right circular cylinders. When the cylinders are in the SmA layer with the long axes along the layer normal, the excluded *area* is

$$A_A = 4\pi R^2 \tag{6.24}$$

where R is the radius of cross section of the cylinders. When the axes of the cylinders are tilted at a small angle ω with respect to the layer normal, as in the SmC layer, the excluded area is increased to

$$\begin{aligned} A_C &= 4\pi R^2/\cos\omega \\ &= 4\pi R^2(1-\sin^2\omega)^{-1/2} \\ &\approx A_A\,[1 + (\sin^2\omega)/2] \end{aligned} \tag{6.25}$$

where the higher powers of $\sin\omega$ are ignored. Hence, the increase in the excluded area can be written as

$$\Delta A \propto \sin^2 \omega \tag{6.26}$$

In hard rod models, the increase in the free energy due to hard core interaction is proportional to the excluded volume, which in this case is proportional to ΔA.As we argued earlier (see section 6.6.1), molecular tilt has significance only in presence of a layering order and the tilting potential varies as τ^2. Therefore the relevant contribution of the hard core interaction to the free energy is written as

$$\delta F_{hr} \propto k_B T\, \tau^2 \sin^2 \omega. \tag{6.27}$$

δF_{hr} is entropic in origin and has a positive sign.

Goossens [33, 23] has made an elaborate calculation of the excluded volume effects for ellipsoids, and has shown that, neglecting the higher powers of $\sin\omega$, the contribution of the hard core interaction to the free energy can be written as

$$\delta V_{SmA}(\omega) = A(S)\, \tau^2 \sin^2 \omega. \tag{6.28}$$

where $A(S)>0$ is a function of the orientational order having the dimensions of energy and the brackets $\langle\infty$ denote the thermal average. Goossens [23] has calculated $A(S)$ for ellipsoids of different eccentricities assuming $S = 0.7$. Using the equations given in reference [23], we can show that the value of $A(S)$ changes only by 50% when S is changed from 0.7 to 0.8 for a/b =2, while it changes by an order of magnitude when a/b is changed from 1.5 to 2 for S =0.7, where a and b are the lengths of the major and minor axes of the ellipsoid representing the molecule. In view of this, we ignore the dependence of $A(S)$ on S and write,

$$\delta F_{hr} = \gamma\, k_B T\, \tau^2 \sin^2 \omega. \tag{6.29}$$

where $\gamma>0$ is a parameter depending on the dimensions of the ellipsoid.

We now adopt the technique developed by Katriel and Kventsel [41] to propose a mean field theory of the smectic C liquid crystal.

6.6.4 Molar internal energy

Using the single particle potentials U_C and U_M given above, the molar internal energy is written as:

$$U = -(N/2)\, U_o\, (1+ \alpha\, \tau^2)\, S^2 - (N/2)\, U_o\, \alpha\, \beta\, \tau^2\, \eta^2 \tag{6.30}$$

where N is the Avogadro number, and the factor (1/2) arises from the fact that each intermolecular energy is counted twice in the averaging process. Note that U_o represents the strength of the orienting potential, $U_o\alpha$ the strength of the layering potential of the orientationally ordered molecules and $U_o\alpha\beta$ the strength of the tilting potential of the molecules having layering order.

6.6.5 Entropy

The molar entropy is

$$\mathcal{S} = -Nk_B \left[\frac{1}{2\pi d} \int_{-1}^{+1} d\cos\theta \int_{0}^{\pi} d\phi \int_{-d/2}^{+d/2} dz\, f \ln f + \gamma\, \tau^2 \sin^2 \omega \right]. \tag{6.31}$$

in which the first term arises from the single particle distribution function $f(\theta,\phi,z)$ and the second term is the hard rod contribution given in equation (6.29).

6.6.6 Molar Helmholtz free energy and the order parameters

The molar Helmholtz free energy is given by

$$F = U - T\mathcal{S}. \tag{6.32}$$

The free energy is now minimised with respect to $f(\theta, \phi, z)$ by a variational procedure to get

$$f = Z^{-1} \exp\{(U_o/k_B T)[(1 + \alpha\tau^2) S (3\cos^2\psi - 1)/2 + \alpha\beta\tau^2\eta \sin 2\theta \cos\phi]$$
$$+ [(U_o/k_B T)\alpha(S^2 + \beta\eta^2) - 2\gamma\sin^2\omega]\tau\cos(2\pi z/d)\} \tag{6.33}$$

where Z is the normalising integral, and the last term involving $\gamma \sin^2\omega$ is clearly athermal in origin. It can be verified that the entropy calculated using $\mathcal{S} = -(\partial F/\partial T)_V$ is the same as that given by equation 6.31. As the nematic director makes a tilt angle ω with the layer normal in the Z-X plane,

$$\cos\psi = \cos\theta\cos\omega + \sin\theta\sin\omega\cos\phi. \tag{6.34}$$

The order parameters, obtained as the averages over the distribution function are

$$S = \frac{1}{2\pi d}\int_{-1}^{+1} d\cos\theta \int_0^{\pi} d\phi \int_{-d/2}^{+d/2} dz\, f.(3\cos^2\psi - 1)/2, \tag{6.35}$$

$$\tau = \frac{1}{2\pi d}\int_{-1}^{+1} d\cos\theta \int_0^{\pi} d\phi \int_{-d/2}^{+d/2} dz\, f.\cos(2\pi z/d), \tag{6.36}$$

$$\eta = \frac{1}{2\pi d}\int_{-1}^{+1} d\cos\theta \int_0^{\pi} d\phi \int_{-d/2}^{+d/2} dz\, f.\sin 2\theta\cos\phi. \tag{6.37}$$

These self-consistency equations also minimise the free energy.

6.6.7 The parameters of the model and their values

The parameters of the model are U_o, α, β and γ. As explained in chapter-2, the value of U_o fixes T_{NI} and is irrelevant since temperatures are expressed as reduced temperatures $T_R = T/T_{NI}$. Hence, the independent parameters are α, β and γ. The value of the McMillan parameter α can vary between zero and 2. The value of $(\alpha\beta)$ is estimated using the calculated interaction energy minima in section 6.5 (see figure 6.16). The calculations in section 6.5 correspond to the medium having perfect order.

With $\tau = \eta = 1$ in equation 6.30, the contribution of the internal energy per molecule from the tilting potential is

$$U_T/k_B T = -U_o \alpha\beta/(2k_B T). \quad (6.38)$$

Using the Maier Saupe value, we have $(U_o/k_B T) = 4.541/T_R$, and with $U_T = U(\omega)$ we get,

$$(\alpha\beta) = -[U(\omega)/k_B T](2T_R/4.541). \quad (6.39)$$

Taking the maximum $T_R \approx 1.5$, and lowest minimum in $U(\omega) \approx -2\ k_B\ T$, the maximum value of $(\alpha\beta) \approx 1.5$ and the minimum value of $(\alpha\beta)$ is obviously zero. Values of the function $A(S)$ are given in ref. [23] up to $a/b = 1.5$, where a and b are the lengths of the major and minor axes of the ellipsoid representing the molecule. We extrapolate these values to find $A(S)$ for $a/b > 1.5$. The value of γ is then estimated using the equations 6.28 and 6.29. As mentioned earlier, the value of γ has a strong dependence on the ratio a/b. We get, $\gamma \sim 1$ for $a/b = 1.5$, $\gamma \sim 10$ for $a/b = 2$ while $\gamma \sim 400$ for $a/b = 3$.

6.6.8 Method of calculation

In our model, η is the order parameter for the SmC phase. But ω, which is the average of the tilt angles θ of individual molecules, is measured in experiments (see section 6.3). ω explicitly appears in our model in equation 6.34. As such, the free energy depends on ω, we minimise F with respect to ω also. This is done as follows. For a set of values of T_R, α, β and γ, some value of ω is assumed in the smectic C phase, and S, τ and η are evaluated satisfying the self consistency of the equations 6.35-37 and F is calculated using equation 6.32. The procedure is repeated for different values of ω to find the free energy minimum with respect to ω. The necessary integrals are evaluated using a 32-point Gaussian qudrature technique under double precision. As can be expected, the variation of ω follows closely that of η. For Small values of η, one can expect $\omega \approx (\eta/2)$ radian (see equation 6.37). The solutions corresponding to the different phases are:

(a) isotropic: $\eta = \tau = S = 0$; (b) nematic: $\eta = \tau = 0$, $S \neq 0$;

(c) smectic A: $\eta = 0$, $\tau \neq 0$, $S \neq 0$ and (d) smectic C: $\eta \neq 0$, $\tau \neq 0$, $S \neq 0$.

The stable phase corresponds to the one which gives the lowest free energy.

6.7 Results and discussion

6.7.1 Typical phase diagrams

The calculated phase diagrams as functions of α and β are shown in figure 6.17 for γ=3. The SmC-SmA transition is second ordered in nature. As α is increased, the SmA range decreases to zero, giving rise to a first order SmC-N transition (figure 6.17a). As explained in chapter-3, an increase of the McMillan parameter α corresponds to an increase of chain length in a homologous series or an increase of the concentration of the longer homologue in a binary mixture. The trend shown in figure 6.17a agrees with that seen in experiments on homologous series (see figure 6.4 and 6.5) or mixtures [42]. There is a small change of slope between the N-SmA and N-SmC transition lines (not clearly seen in the figure 6.17a). An increase of β alone corresponds to an increase of tilting potential without changing the chain length. As discussed in our illustrative calculations of dipolar interactions (section 6.5.7), this increase can be the result of changing the number and/or the relative locations of the dipoles. It is known that [8, 9] the addition of an extra dipole to the molecular structure changes the N-SmA-SmC phase sequence to N-SmC sequence (see section 6.5.8 for details). This trend is seen as β is increased in figure 6.17b.

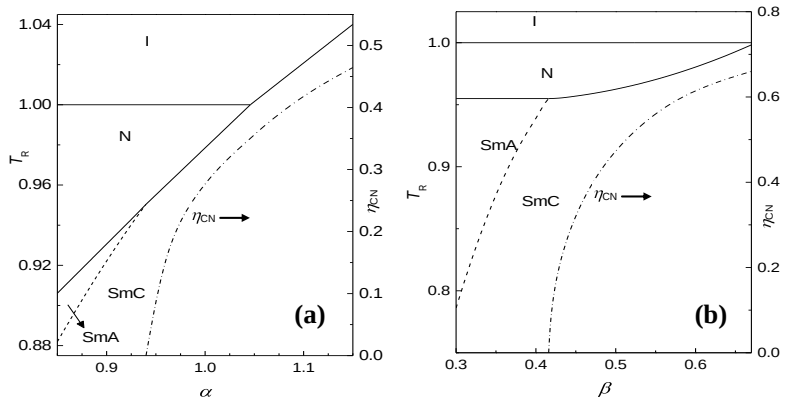

Figure – 6.17. Calculated phase diagrams for γ = 3, (a) as a function of α with β = 0.42 and (b) as a function of β with α =0.95. The dashed line indicates a second order transition and the solid line indicates a first order transition. The jump in η at the first order SmC-N transition decreases to zero as the N-SmA-SmC point is reached.

6.7.2 Variation of order parameters and specific heat with temperature

The phase diagram obtained for β = 0.4, and γ =3 is similar to that shown in figure 6.17a. In this range of parameters, for α = 0.95, the SmC-N transition is first ordered in nature. As the N-SmA-SmC meeting point is approached, the jump in η (and ω) across the SmC-N transition reduces to zero. The SmA-SmC transition is second ordered in nature, with the relevant order parameter η increasing from 0 as the temperature is lowered from T_{AC}. The calculated tilt angle ω also shows a similar trend (Figure 6.18a). Note that only the tilt angle ω is measured in experiments [10] and not the order parameter η. We have also numerically estimated the specific heat at constant volume (C_V) close to the SmA-SmC transition point using the internal energy versus temperature plot. The calculated jump in C_V across the SmC-SmA transition is shown in figure 6.18b. ΔC_V is of the same order of magnitude as that obtained in experiments [43] for ΔC_P.

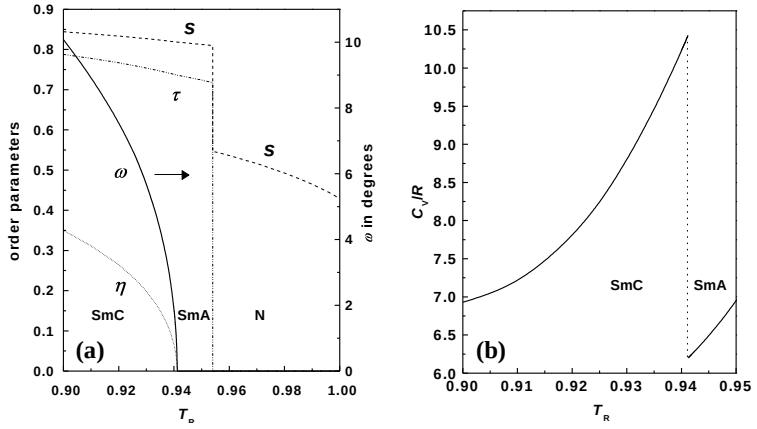

Figure – 6.18. (a) Temperature variations of the order parameters *S*, τ, η and the tilt angle ω for α = 0.95, β = 0.4 and γ = 3.(b) Jump in the specific heat at constant volume C_V expressed in terms of the universal gas constant *R*, across the SmC-SmA transition point shown in (a).

6.7.3 Tricritical behaviour

As already explained in chapter-3, when α is increased, the nature of SmA-N transition changes from 2nd order to 1st order (tricritical behaviour). For the SmA-N transition, the tricritical point (t.c.p) is at α = 0.5112 and at T_R = 0.7034 [41]. In the present calculations, we get a tricritical behaviour of the SmC-SmA transition for β=1

and $\gamma = 5$ (t.c.p at $\alpha = 0.521$ and $T_R = 0.700852$). The T_R-α phase diagram containing both the SmA-N as well as SmC-SmA tricritical points is shown in figure 6.19a. When the value of β is increased to 1.2 and γ to 12, the SmC-SmA t.c.p appears at a higher value of α (t.c.p at $\alpha = 0.77$ and at $T_R = 0.83441$). On increasing the values of β and γ further, the SmC-SmA t.c.p appears at a still higher value of α (with $\beta = 1.45$ and $\gamma = 50$, t.c.p at $\alpha = 1.09$ and at $T_R = 0.97309$, see figure 6.19b). Larger values of γ corresponds to molecules having larger length to width ratios, as explained in section 6.6.7.

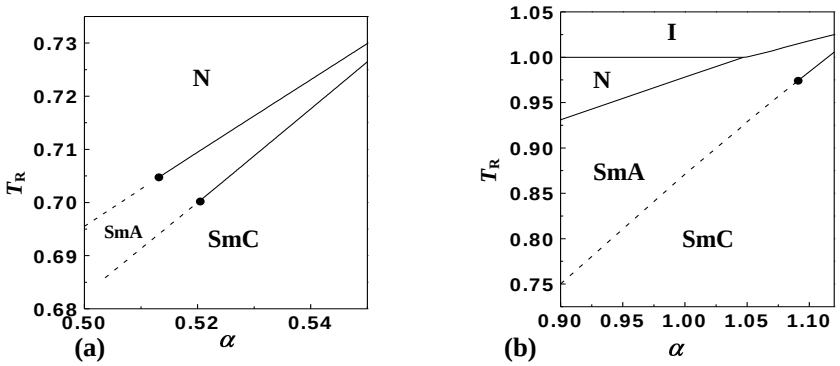

Figure - 6.19. Phase diagrams as functions of α for (a) $\beta = 1$, $\gamma = 5$ and (b) $\beta = 1.45$, $\gamma = 50$. The dashed lines indicate second order transitions. The tricritical points are shown by filled circles.

The SmA temperature range decreases when α is increased. This trend is seen in the experiments [11], as already described in section 6.3.4 (see table 6.1).

As the SmA-SmC t.c.p is approached, the calculated temperature variation of ω becomes steeper (figure 6.20). As discussed in section 6.4.1, the experimental results are often analysed using the Landau free energy density

$$F_C = a\,(T - T_{AC})/T_{AC}\;\; \omega^2 + b\omega^4 + c\omega^6 \qquad (6.40)$$

with a relatively large *c*-coefficient. Our expression for the free energy can not be directly expanded in this form since all the terms in the expansion of the exponential function in equation 6.33 contribute to different powers of ω. Hence, we have numerically fitted the calculated F and ω values to this functional form for temperatures $T/T_{AC} > 0.98$ to find b/a and c/a. As the SmA-SmC t.c.p is approached, the coefficient c becomes relatively large compared to b and hence the value of t_o (see

equation 6.5) decreases. Also the jump in the specific heat across the transition point increases. Some values showing this trend are given in table 6.3 for $\beta = 1$ and $\gamma = 5$ (SmA-SmC t.c.p at $\alpha = 0.521$ and $T_R = 0.700852$, see figure 6.19a). A similar trend is also seen experimentally. A detailed study on various compounds by Huang and Lien [44a] showing this trend is summarised in table 6.4. Experimentally a value of t_0 as small as 10^{-5} has been found in a compound [44b].

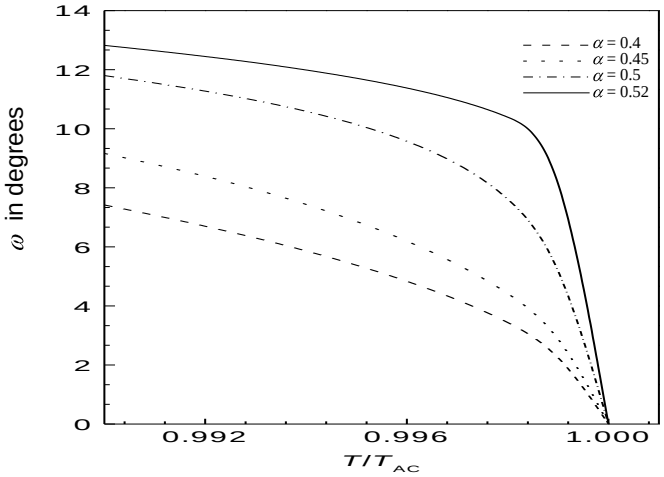

Figure – 6.20. Diagram showing the temperature variation of ω becoming steeper as the SmA-SmC t.c.p in figure 6.19a is approached.

Table 6.3. Various parameters close to t.c.p, calculated theoretically.

α	ω at $T_{CA}-T = 4^0$C	b/a	c/a	SmA range $1-(T_{CA}/T_{AN})$	t_0 $=b^2/(ac)$	$\Delta C_V/R$
0.4	7.4^0	0.27	1.3	0.046	5.6×10^{-2}	7
0.45	9.2^0	0.15	1.26	0.032	1.8×10^{-2}	15
0.48	10.7^0	0.06	1.2	0.024	3×10^{-3}	29
0.5	11.8^0	0.03	1	0.0185	9×10^{-4}	49
0.52	12.8^0	0.0025	0.3	0.013	2.1×10^{-5}	186

The second column gives ω at $T_R = 0.99T_{CA}/T_{NI}$, *i.e.*, at $T_{CA} - T = 4^0$C taking $T_{CA}\approx400$K. Note the decrease in the value of t_0 and the increase in the specific heat jump as the t.c.p is approached.

Table 6.4. Experimental values [45] close to t.c.p.

Compound	SmA range $1-(T_{CA}/T_{AN})$	$t_0 \times 10^3$	ΔC J/molK
2M4P9OBE	0.077	5.5	134
7O.7	0.034	2.8	123
7O.4	0.027	0.8	400
2M45OBC	0.062*	3.9	124
DOBAMBC	0.058*	3.2	125
7O.6	0.029*	1.6	258

Experimental values showing the decrease in the value of t_0 and the increase in the specific heat jump ΔC as the t.c.p is approached. The values with an asterisk correspond to $1-(T_{CA}/T_{AI})$.

Our calculations show that the t.c.p can also be approached by increasing β alone. With $\alpha = 0.521$ and $\gamma = 5$, the SmC-SmA transition is second ordered in nature for $\beta < 1$ and changes to first order at $\beta = 1$. An increase of β corresponds to an increase of the strength of the dipole moments of the constituent molecules. This trend is seen in binary mixtures of compounds, one with weak and the other strong dipole moments [14]. As the relative concentration of the strongly polar compound is increased, the temperature range of SmA decreases and the second order SmC-SmA transition changes to first order. As noted by Liu *et al*, [15] this can be interpreted as due to an increase in the *effective* molecular transverse dipole moment.

6.7.4 Effect of variation of γ

The value of γ determines the stability of the layers against molecular tilt (see section 6.6.3). The T_R-γ phase diagram for $\alpha = 0.9$, $\beta = 0.4$ is shown in figure 6.21. As γ increases, the SmA phase becomes more stable than the SmC phase and the SmA range increases.

When γ is small, *i.e.*, when the length to breadth ratio of the molecules is small (see section 6.6.7), even at large values of α and relatively small values of β the SmC phase is stabilised. In this case, the SmC phase can undergo a strong first order

transition to the nematic phase. The tilt angle in such a smectic C is quite large (~40^0), and hardly varies with temperature as shown in figure 6.22 for α = 0.97, β = 0.1, γ=0.15. These trends are known in the literature [45].

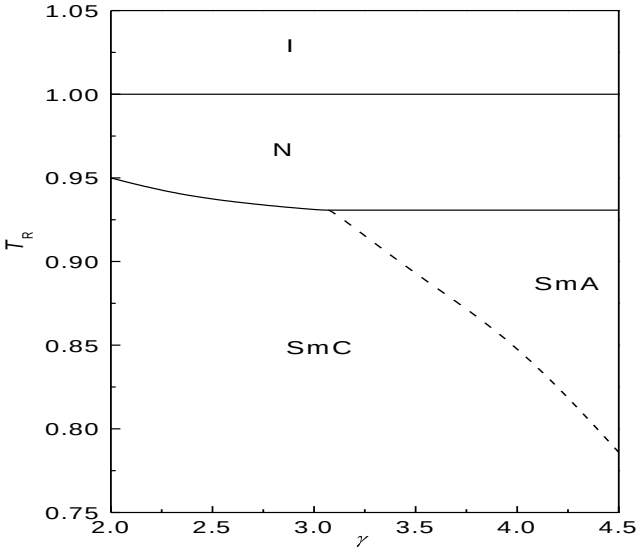

Figure – 6.21. Calculated phase diagram as a function of γ for α = 0.9, β = 0.4. The dashed line indicates a second order SmC-SmA transition.

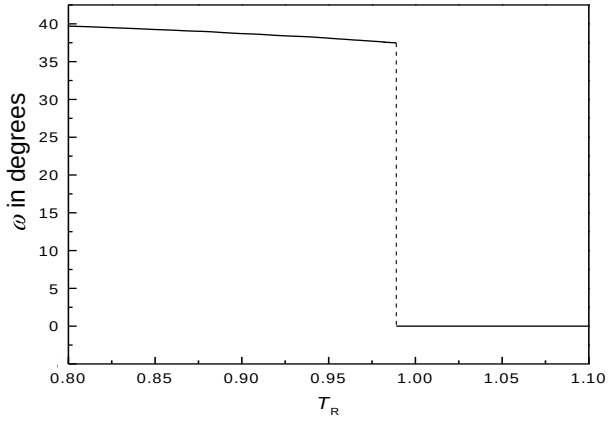

Figure – 6.22.Temperature variation of ω at a strong first order SmC-N transition for α = 0.97, β = 0.1, γ = 0.15.

Some other types of phase diagrams are obtained when the parameters of the model are varied. These are discussed in the next section.

6.7.5 Other possible phase diagrams

For β = 0.495 and γ = 2, we get a phase diagram showing the N-SmA-SmC meeting point at α = 0.5112 and at T_R = 0.7034 (figure 6.23) where the second order SmC-SmA and SmA-N transition lines meet the first order SmC-N transition line. As the value of α is decreased towards the N-SmA-SmC point, the first order character of the SmC-N transition becomes weaker and finally it becomes second ordered *at* the meeting point. Such a point is called a Lifshitz point [46].This behaviour is seen in an experiment [47] on the binary mixture of pentyloxyphenyl octyloxy benzoate ($\overline{5}$ O $\overline{8}$) and its higher homologue $\overline{6}$ O $\overline{8}$, as the concentration of the longer homologue is decreased. Note that a decrease in the concentration of the longer homologue in a binary mixture is equivalent to a decrease in the value of α in our model. Also, this behaviour is predicted by the phenomenological model of Chen and Lubensky [20]. Precise measurements on several binary mixtures [48] and high pressure studies on a single component system [49] show that the N-SmA-SmC meeting point is a multicritical point with a universal topology. A theoretical description of this topology would involve the consideration of the fluctuations in the relevant order parameters. This is beyond the scope of our molecular mean field theory.

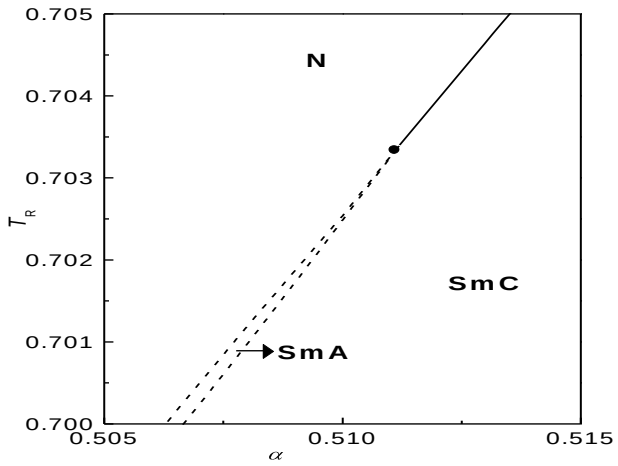

Figure – 6.23. Calculated phase diagram for γ = 2 and β = 0.495, showing the second order SmC-SmA and SmA-N transition lines meeting the first order SmC-N transition line at α = 0.5112. The meeting point is shown by a filled circle and the second order phase transitions are shown by dashed lines.

When the value of β is increased to 0.499995 with $\gamma = 2$, the SmC-N transition becomes second ordered in nature for $\alpha < 0.510275$ (as will be discussed later). With these values for β and γ, when the value of α is further decreased, we get the N-SmA-SmC point at $\alpha = 0.502$ and $T_R = 0.696839$ where the three second order transition lines meet. The SmC-SmA and the SmA-N transition lines are rather close by and the range of SmA is very much smaller than that in figure 6.23 and can not be conveniently shown in a diagram. We have not come across any experimental study of this type of a meeting point.

6.7.6 SmC-SmC transition

As mentioned in the previous section, the first order SmC-N transition becomes second ordered in nature at $\alpha = 0.510275$ and $T_R = 0.702738$, with $\beta = 0.499995$ and $\gamma = 2$. A very unusual behaviour is seen when α is slightly lower. For a very narrow range of values of $\alpha < 0.510275$, as the temperature is decreased across T_{CN}, initially ω continuously increases from zero, but *jumps* to a higher value below some temperature *i.e.*, we get a first order SmC-SmC transition (see figure 6.24).

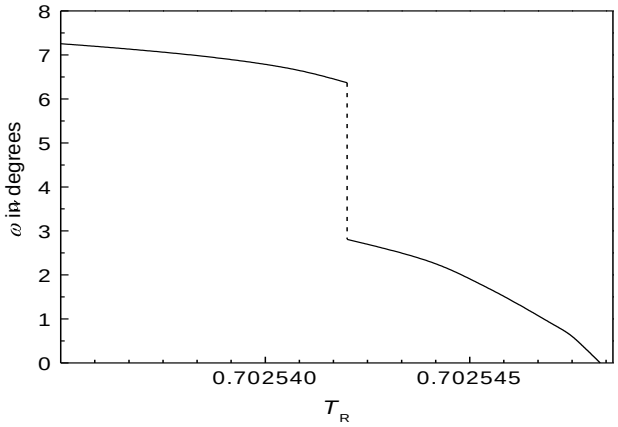

Figure – 6.24. Diagram showing a jump in ω at a SmC-SmC transition for $\alpha = 0.5100$, $\beta = 0.499995$ and $\gamma = 2$.

The SmC-SmC transition occurs at a temperature which is only a few millikelvin below the second order SmC-N transition. The transition becomes weaker as α is decreased and finally ends in a critical point (at $\alpha = 0.50986$ and $T_R = 0.702442$) at which the jump in ω becomes zero. The phase diagram with the SmC-SmC transition

line ending in a critical point is shown in figure 6.25a and the corresponding variation of ω with α is shown in figure 6.25b. We have not come across any experimental observation in support of the SmC-SmC transition. However, in SmC* liquid crystals an electric field induced first order SmC - SmC transition has been observed [50]. In SmA liquid crystals composed of chiral molecules, a tilt angle can be induced by an external electric field (electroclinic effect) and a large electric field unwinds the helix in SmC* liquid crystals. Experimentally, a first order transition between these two 'SmC' phases ending in a critical point as a function of electric field has been investigated [50]. A discussion of this type of transition is beyond the scope of our theory.

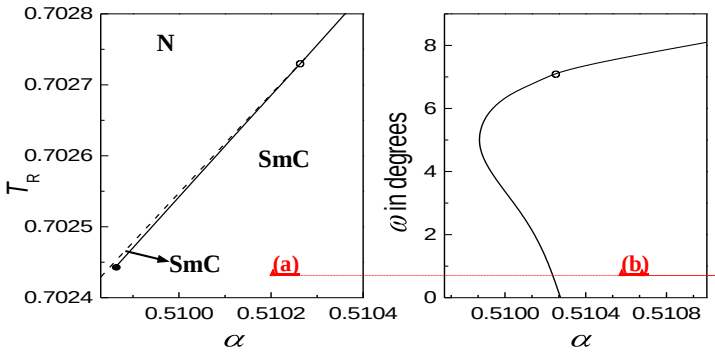

Figure – 6.25. (a) Calculated phase diagram for β =0.499995 and γ= 2, showing the first order SmC-SmC transition line ending in a critical point (shown by a filled circle). The dashed line indicates a second order SmC-N transition. The calculated variation in ω corresponding to the SmC-SmC and the SmC-N transitions is shown in (b). Note that for α<0.510275, there are two values of ω indicating a jump in ω at the SmC-SmC transition. Above this value of α, ω jumps to zero at the first ordered SmC-N transition. The hollow circle in both (a) and (b) corresponds to the point where the SmC-SmC transition line branches off.

6.8 Some extensions of the model

6.8.1 Inclusion of a higher order term in the tilting potential

For simplicity we have carried out the above calculations restricting *n* to 1 in the general form of the potential written in equation 6.22 and this favours a maximum tilt angle of 45^0. It is known in a few cases [3] that the maximum tilt angle can be > 45^0. This can be incorporated including the next term *i.e.*, $\sin 2n\theta\cos\phi$ with n = 2, with a small negative coefficient. We have extended our calculations with

Formatted
Formatted
Formatted

$$U_C(\theta_i, \phi_i) \propto -\tau^2(\beta_1 \eta_1 \sin 2\theta_i \cos \phi_i + \beta_2 \eta_2 \sin 4\theta_i \cos \phi_i) \quad (6.41)$$

where β_n, τ, η_n, θ_i and ϕ_i have the same meaning as in equation 6.22.

The T_R -α phase diagram with $\beta_1 = 0.4$, $\beta_2 = -0.05$, $\gamma = 3$ is shown in figure 6.26a and the temperature variation of the order parameters η_1 and η_2 as well as those of s, τ and ω are shown in figure 6.26b.

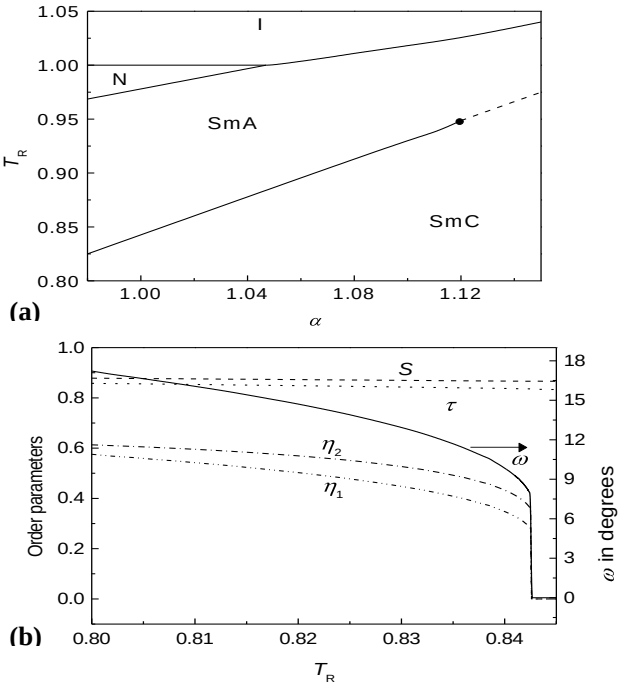

Figure – 6.26. (a) Calculated phase diagram for $\beta_1 = 0.4$, $\beta_2 = -0.05$, $\gamma = 3$. The second order transition is shown by a dashed line and the filled circle indicates the t.c.p. (b) The temperature variation of the order parameters and ω near the first order SmC-SmA transition corresponding to figure (a) at $\alpha = 1$ and $T_R = 0.8425$.

As α increases, the nature of the SmC-SmA transition changes from first order to second order at the t.c.p. Note that this trend is opposite to that shown in figure 6.19 where $\beta_2 = 0$. We can compare this with a trend seen [44a] in a binary mixture of pentylphenylthiol - octyloxybenzoate (denoted as $\overline{8}$S5) and its lower homologue $\overline{7}$S5. As the relative concentration of $\overline{7}$S5 is increased, which is equivalent to decreasing α in our calculations, the value of t_0 for the second order SmC-SmA transition decreases. This shows that the t.c.p is being approached as explained in section 6.7.3.

6.8.2 Different tilts of core and chain

While carrying out the above calculations, for simplicity we have assumed that the core and the chain tilt with the same angle ω with respect to the layer normal. It is known that [6] the two tilts are not necessarily the same. Hence, in the SmC phase, the effective value of α depends on ω. The McMillan parameter is given by

$$\alpha = 2\exp[-(\pi r_0/d)^2] \tag{6.42}$$

where r_0/d is the ratio of the length of the core to the layer spacing. Considering the molecules with symmetric end chains of length c each, when the core and the chains have the same tilt angle ω, the layer spacing in the SmC liquid crystals

$$d_C = (r_0 + 2c)\cos\omega \tag{6.43}$$

and the effective core length

$$r_{0C} = r_0\cos\omega. \tag{6.44}$$

This leads to α_0 same as α in equation 6.42.

When the core tilt angle (ω_{CR}) is larger than the chain tilt angle (ω_{CH}), the effective core length decreases thus increasing the effective value of α. We have,

$$d_C = r_0\cos\omega_{CR} + 2c\cos\omega_{CH} \tag{6.45}$$

and the effective core length

$$r_{0C} = r_0\cos\omega_{CR}. \tag{6.46}$$

With this, assuming $\omega_{CR}/\omega_{CH} = 1.5$, we have calculated α/α_o for different values of ω_{CR}. Using a polynomial fit to the plot of α/α_o vs ω_{CR}, we get the first order correction as

$$\alpha = \alpha_o(1 + K\omega^2), \tag{6.47}$$

with K $\approx$ 0.3 when $\alpha_o \approx 1$. The T_R -α_0 phase diagram obtained including this correction is shown in figure 6.27, for $\beta_1 = 0.36$, $\beta_2 = 0$ and $\gamma = 3$. Note that the topology of the phase diagram is the same as that in figure 6.17a, while the slopes of the SmC-N and the SmC-I transition lines have increased.

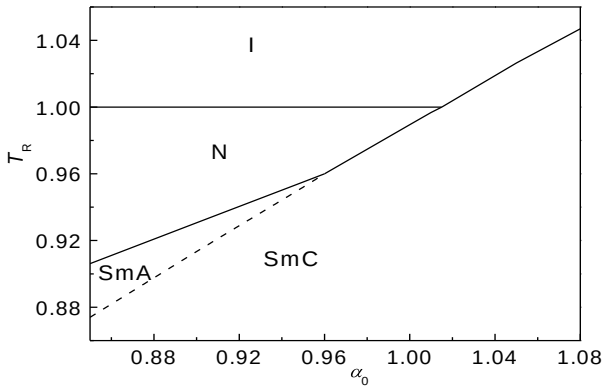

Figure - -6.27. Calculated phase diagram for β_1 = 0.36, β_2 = 0, γ =3 and K = 0.3. The dashed line indicates the second order transition.

6.8.3 Other possible extensions

The following extensions of the model are possible:

1. The length of the end chains c_1 and c_2 can be considered to be unequal. As in the previous chapters, this leads to different values of effective α and pairing energy for antiparallel and parallel pairs. The model can be extended to include this difference.
2. Interlayer and chiral interactions can be considered. Including this, the model can be extended for SmC_{alt} and SmC* liquid crystals.
3. The interaction between the longitudinal components of the dipole moments and also the chains of the molecules can be included. Considering antiparallel and parallel pairs, as in the previous chapters, the model can be extended to describe transitions between SmC_1, SmA_1, SmC_d, SmA_d, N_1 and N_d phases.
4. The hard rod excluded volume contribution to the free energy needs a more rigorous calculation.

6.9 Conclusions

We have demonstrated that the *off-axis* character of the lateral dipolar groups can account for tilt in layered smectics (SmC, SmC*, SmI *etc*.). We have used the simplest single particle potential consistent with the symmetries of the SmC phase to develop a mean field theory [51], including the hard rod features which stabilise the

SmA phase. The topology of the calculated phase diagrams involving isotropic, nematic, SmA and SmC phases, temperature variation of tilt angle in the SmC phase, the specific heat jump across the SmA-SmC transition and the appearance of a tricirtical point as the SmA range decreases compare favourably with experimental trends. Also, a first order SmC to SmC transition is found to occur over a very small range of values of α, β and temperature. The calculations have been extended to include the next higher order term in the tilting potential and to include the effect of different tilt angles for the core and the chain in the SmC phase. Some possible extensions of the model have been pointed out.

6.10 References for chapter-6

[1] Goodby, J. W., and Gray, G. W., *Smectic Liquid Crystals : Textures and Structures*, Leonard Hill, Heyden and Son, Inc, Philadelphia, 1984.

[2] Sackmann, H., and Demus, D., *Mol.Cryst.Liq.Cryst*, **2**, 81, 1966.

[3] P.G.DeGennes and J.Prost, *The Physics of liquid crystals*, 2nd edition, Clarendon press, Oxford, 1993.

[4] Tuffin, R. P., Goodby, J. W., Bennemann, D., Heppke, G., Lotszch, D., and Scherowsky, G., *Mol.Cryst.Liq.Cryst*, **260**, 51, 1995.

[5] Galerne, Y., Lagerwall, S. T., and Smith, I. W., *Optics communications*, **19**, 147, 1976; Lochart, E. T., Allender, D. W., Gelerinter, E., and Johnson, D. L., *Phys. Rev. A*, **20**, 1655, 1979.

[6] Goodby , J. W., in *Ferroelctric Liquid Crystals*, GOODBY J.W. *et. al*, (Gordon and Breach) 1991, p.99.

[7] (a) Goodby , J. W., in Chapter-5, Vol 2A, *Handbook of Liquid Crystals*, Demus, D., *et al*, (Wiley-VCH, New York),1998.(b) Guillon, D., *ibid*, chapter-2.

[8] de Jeu, W. H, *J.Physique*, **38** , 1265, 1977.

[9] Guillon, D, Stamatoff, J., and Cladis P. E., *J. Chem. Phy*., **76**, 2056, 1982.

[10]Goodby , J. W., in *Ferroelctric Liquid Crystals*, GOODBY J.W. *et. al*, (Gordon and Breach) 1991, p.240.

[11] Krishna Prasad, S., Raja, V. N, Shankar Rao, D., Geetha Nair, G. and Neubert, M. E., *Phys. Rev. A*, **42**, 2479, 1990.

Formatted

Formatted

[12] Wiegleben, A., Richter, L., Deresch,. J., and Demus, D., *Mol.Cryst.Liq.Cryst*, **59**, 329, 1980.

[13] Heinrich,B., and Guillon, D., *Mol.Cryst.Liq.Cryst*, **268**, 21, 1995.

[14] Shashidhar, R., Ratna, B. R., Geetha Nair, G.,Krishna Prasad, S., Bahr, Ch., Heppke, G., *Phys. Rev. Lett*, **61**, 547, 1988.

[15] Liu, H. Y., Huang, C. C., Min, T., Wand, M. D., Walba, D., M., Clark, N. A., Bahr, C. H. and Heppke, G., *Phys. Rev. A*, **40**, 6759, 1989.

[16] (a)Huang, C. C. and Viner, J. M., *Phys. Rev. A*, **25**, 3385, 1982. (b)Lien S.C. and Huang C. C., *Phys.Rev.A*, **30**, 624, 1984. Note that in Table II, the coefficient *b* should be expressed in 10^{-4} and not 10^{-2}.

[17] ~~Usual mean field~~Ahlers, G., Kornblit., A., and Guggenheim, H. J.,~~,~~ *Phys. Rev. Lett*, **34**, 1227, 1975.

[18] For TCOB (trans-1,4-cyclohexane-di-n-octyloxybenzoate), in Shankar Rao Thesis (Raman Research Institute), Ch.6

[19] Chu, K. C., and McMillan, W. L., *Phys.Rev*, **15A**, 1181, 1977.

[20] Chen, J. and Lubensky, T. C., *Phys.Rev*, **14A**, 1202, 1976; Zeks B and Blinc R., in *Ferroelctric Liquid Crystals*, Goodby J.W. *et. al*, (Gordon and Breach) 1991, p.365.

[21] Maier, W., and Saupe, A., *Z.Naturforsch*, **A14**, 882, 1959.

[22] McMillan, W. L., *Phy. Rev. A*, **4**, 1238, 1971.

[23] Goossens, W. J. A., *Mol.Cryst.Liq.Cryst*, **150**, 419, 1987.

[24]Stroobants, A., Lekkerkerker, H. N. W., and Frenkel, D. , 1986, *Phys. Rev. Lett.*, **57**, 1452; 1987, *Phys. Rev. A*, **36**, 2929.

[25] McMillan, W. L., *Phys.Rev.A*, **8**, 1921, 1973.

[26] Wulf, A., *Phys.Rev.A*, **11**, 365, 1975. A 2-D version of this model has been proposed recently: Vanakaras A. G., Photinos D. J. and Samulsky E. T., *Phys.Rev.E*, **57**, R4875, 1998.

[27] Goodby, J. W., Gray, G. W., and McDonnell, D. G., *Mol.Cryst.Liq.Cryst. Lett*, **34**, 183, 1977.

[28] Luz Z. and Meiboom S., *J. Chem. Phys.*, **59**, 275, 1973.

[29] Dianoux, A. J., Heidemann, A., Volino, F., and Hervet, H., *Mol. Phys.*,**35**, 1521, 1976.

[30] Goossens W. J. A., *J.Physique*, **46**, 1411, 1985.

[31] Cabib, G. and Benguigui, L., *J. Phys.*,**38**, 419, 1977.

[32] Van der Meer, B. W. and Vertogen, G., *J.Physique,Coll*. **40**, C3-222, 1979.

[33] Goossens, W. J. A., *Europhy. Lett*, **3**, 341, 1987.

[34] Barbero, G. and Durand, G., *Mol.Cryst.Liquid.Cryst*, **179**, 57, 1990.

[35] Velasco, E., Mederos, L. and Sluckin, T.G., *Liquid Crystals*, **20**, 399, 1996.

[36] Giesselmann, F. and Zugenmaier, P., *Phys.Rev.E*, **55**, 5613, 1997.

[37] Hu, L. and Tao, R., *Phys.Rev.E*, **58**, 7435, 1998.

[38] Coates, D., *Liquid Crystals*, **2**, 423, 1987.

[39] Van der Meer, B. W., Postma, F., Dekker, A. J. and de Jeu, W. H., *Mol. Phys.*, **45,** 1227, 1982.

[40] Sy, D. and Ptak, M., *J.Physique. lett*, **40**, L-137 1979.

[41] Katriel, J. and Kventsel, G. F., *Phys.Rev.A*, **28**, 3037, 1983.

[42] Goodby, J. W. and Gray, G. W. *J.Physique,Coll.*, **37**, C3-17, 1976.

[43] Birgeneau, R. J., Garland, C. W., Kortan, A. R., Litster, J. D., Meichle, M., Ocko, B. M., Rosenblatt, C., Yu, L. J. and Goodby, J. W, *Phys.Rev.A*, **27**, 1251, 1983.

[44] (a) Huang, C. C., and Lien, S.C. and *Phys.Rev.A*, **31** 2621, 1985.(b) Liu, H. Y., Huang, C. C., Bahr, Ch, Heppke, G., *Phys. Rev. Let.*, **61**, 345, 1988.

[45] Clark, N. A., and Lagerwall, T. S., in *Ferroelctric Liquid Crystals*, Goodby J.W. *et. al*, (Gordon and Breach) 1991, Chapter-1.

[46] Anisimov, M. A., in *Critical Phenomena in Liquids and Liquid Crystals*, (Gordon and Breach) 1991, Chapter 10.

[47] Thoen, J., and Parret, R.,*Liq. Cryst.*, **5**, 479, 1989.

[48] Johnson, D, Allender, D., Richard deHoff, Maze, C., Oppenheim, E and Reynolds. R, *Phys. Rev. B*, **16**, 470, 1977 ; Brisbin, D., Johnson, D. L., Fellner, H., and Neubert, M. E., *Phys. Rev. Lett*, **50**,178, 1983.

[49] Shashidhar, R., Ratna, B. R., and Krishna Prasad, S., *Phys. Rev. Lett*, **53**, 2141, 1984.

[50] Bahr, Ch., and Heppke. G., *Phys. Rev. A*, **41**, 4335, 1990.

[51] Govind, A. S., and Madhusudana, N. V., *Eur. Phys. Lett.*, **55**, 505, 2001.

Formatted